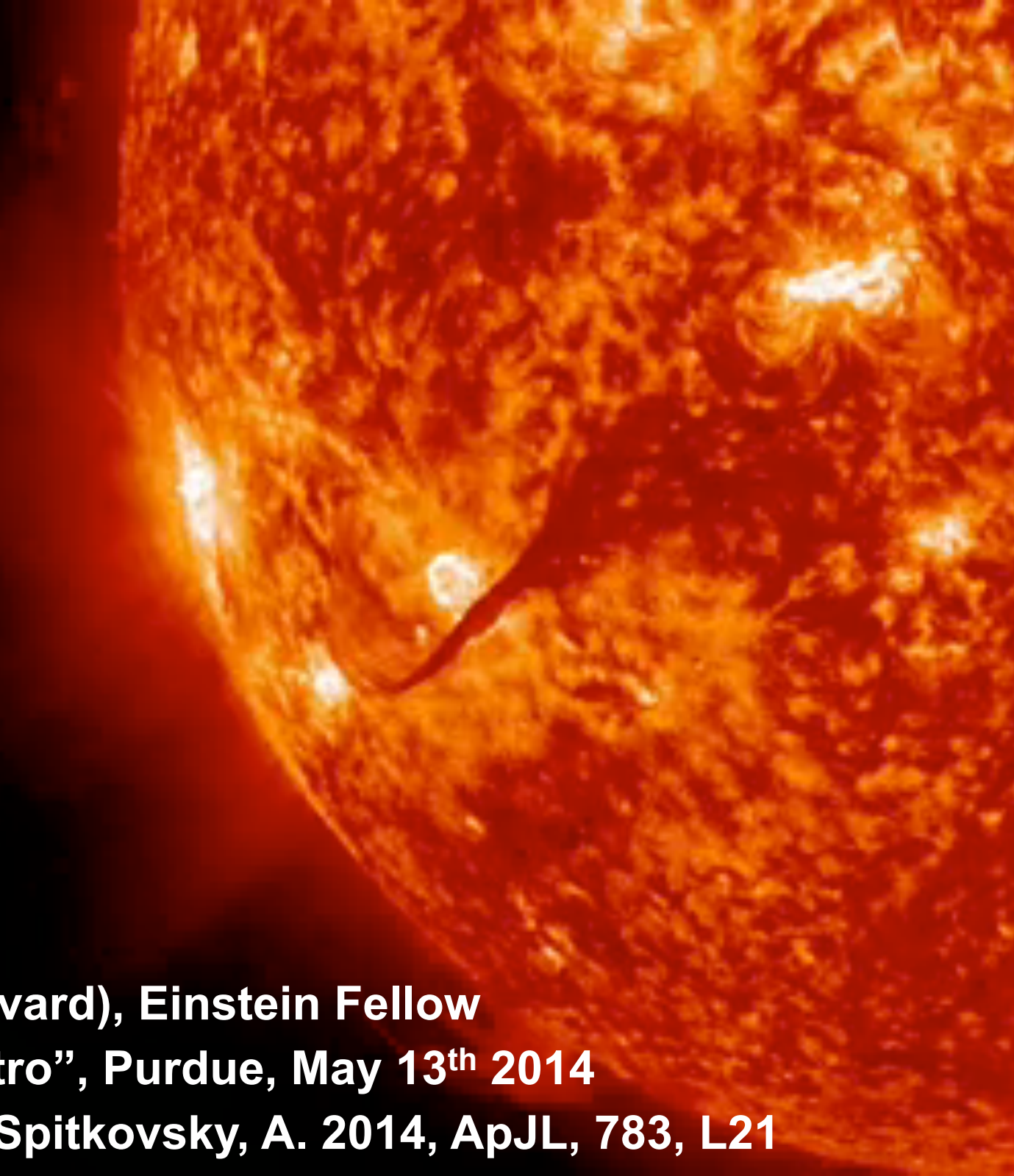


Particle Acceleration by Relativistic Magnetic Reconnection



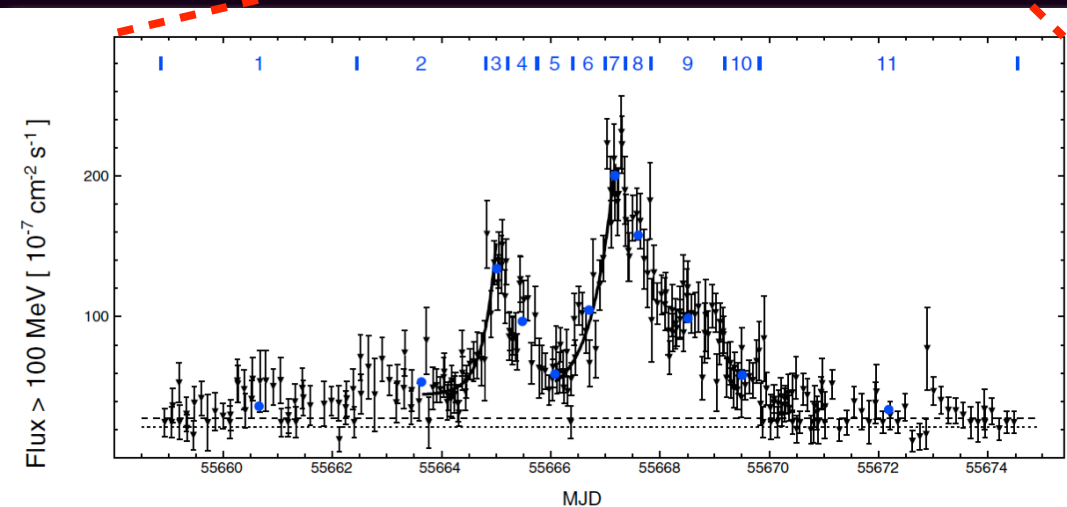
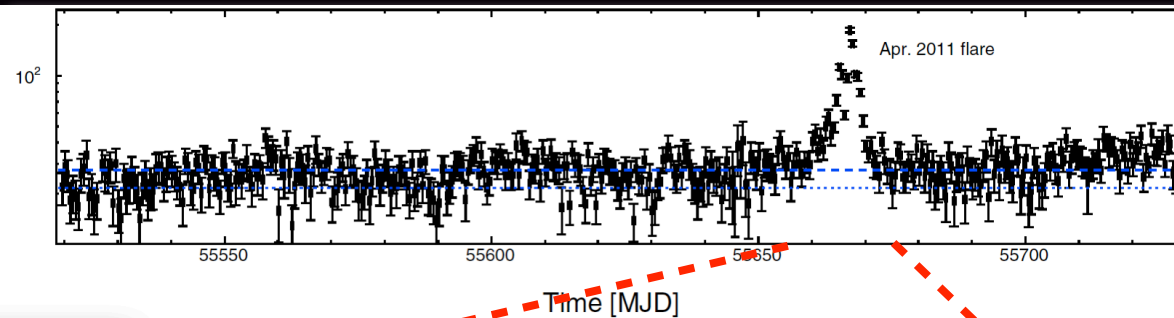
Lorenzo Sironi (ITC-Harvard), Einstein Fellow

“Relativistic Plasma Astro”, Purdue, May 13th 2014

LS 2014, in prep.; LS & Spitkovsky, A. 2014, ApJL, 783, L21

Fast flares in relativistic flows

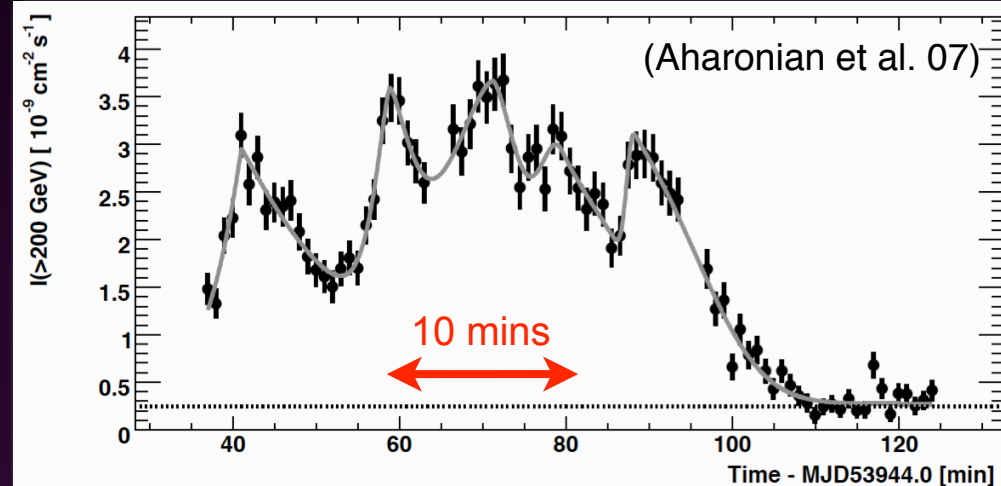
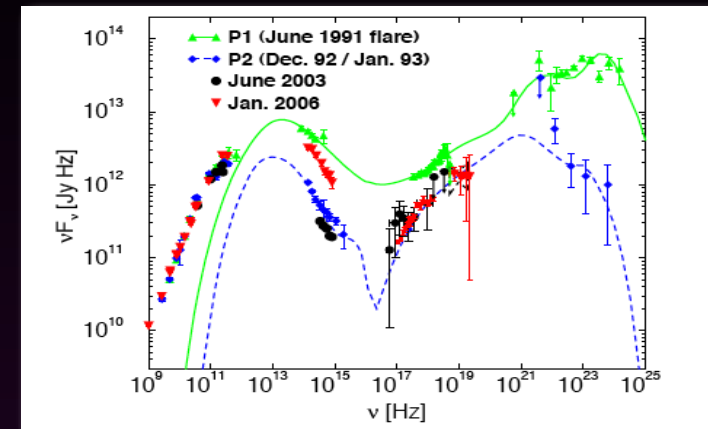
Crab Nebula



(Buehler et al. 12)

Doubling time of ~ 8 hrs, with peak photon flux ~ 30 times larger than the average

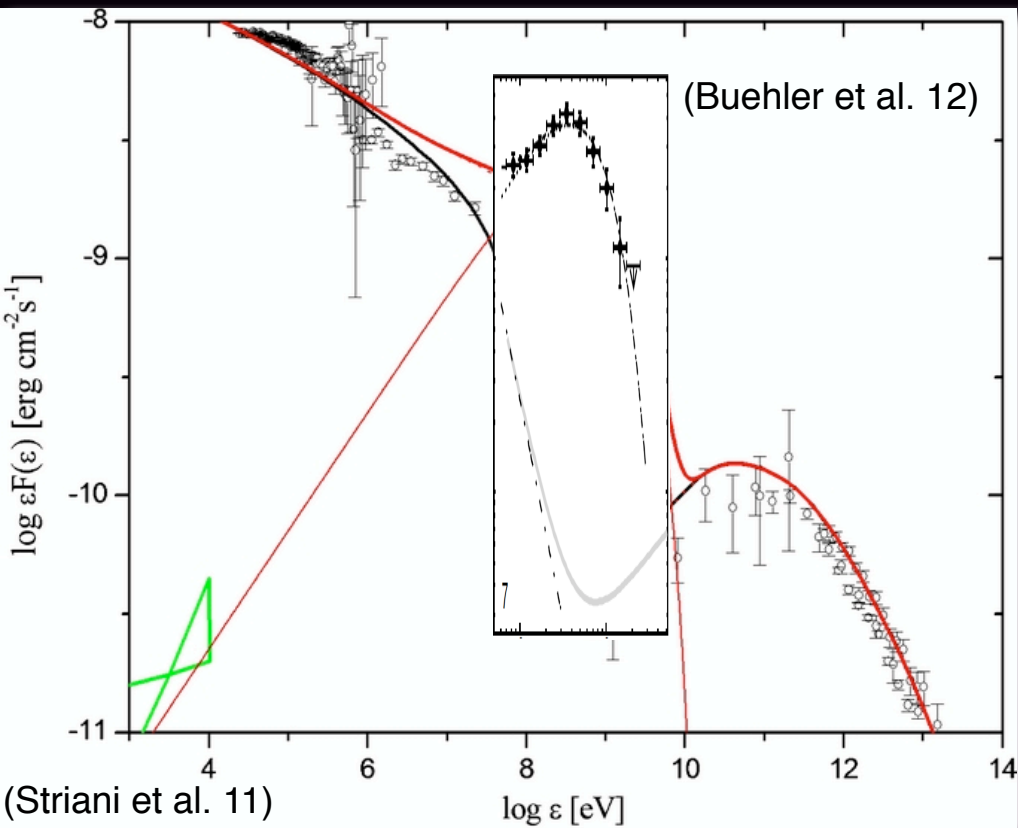
TeV blazars



~ 10 minutes flares on top of a high-state "envelope" that lasts for \sim days

Hard spectra in relativistic flows

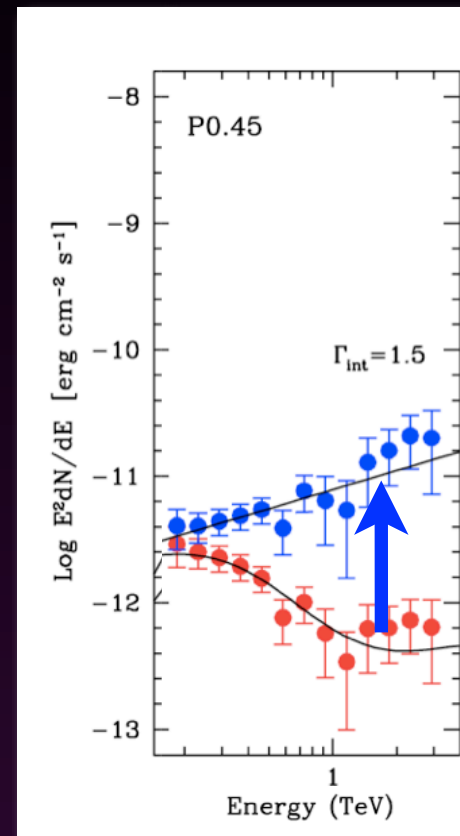
Crab Nebula



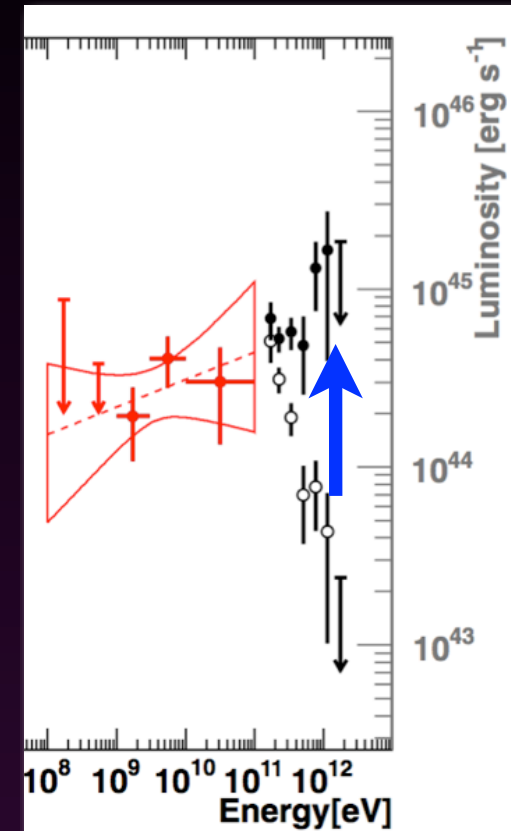
The flare spectrum below the peak

requires $p < 2$. $\frac{dn}{d\gamma} \propto \gamma^{-p}$

TeV blazars



(Aharonian et al. 06)



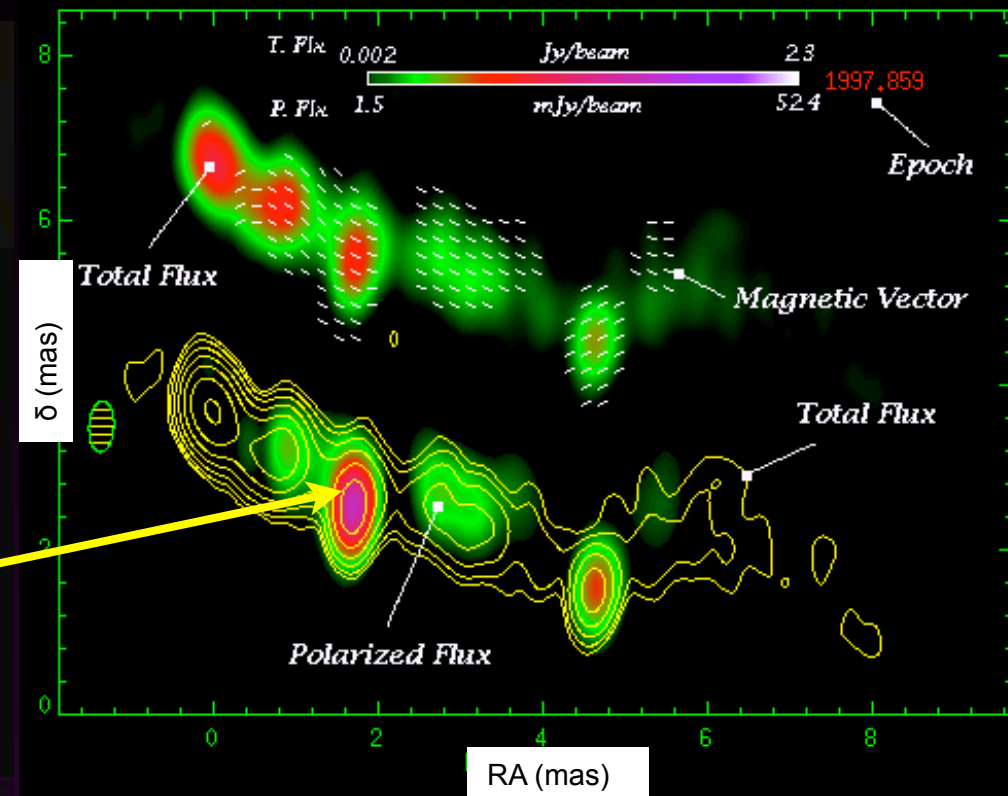
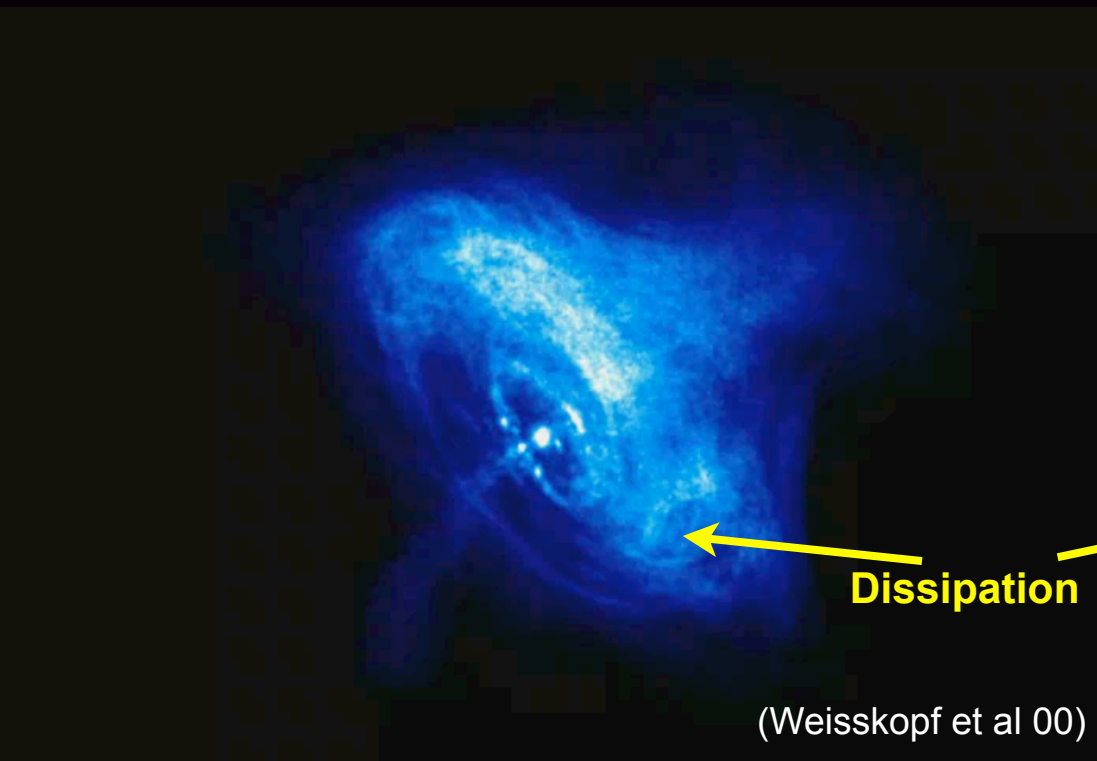
(HESS 11)

After correcting for EBL absorption, the inferred TeV spectra are extremely hard (requiring $p < 2$).

Dissipation in relativistic outflows

Crab Nebula

3C 120

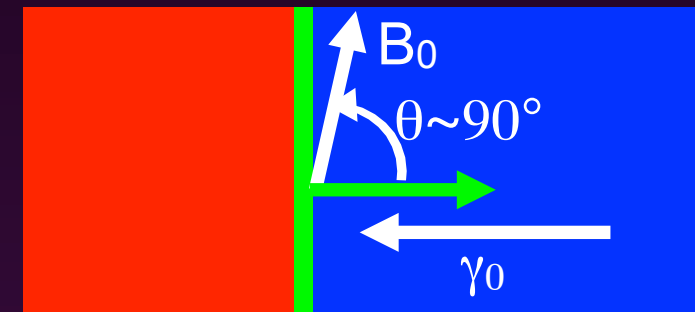


Relativistic outflows: $\gamma_0 \gg 1$

Magnetized: $\sigma > 0.01$

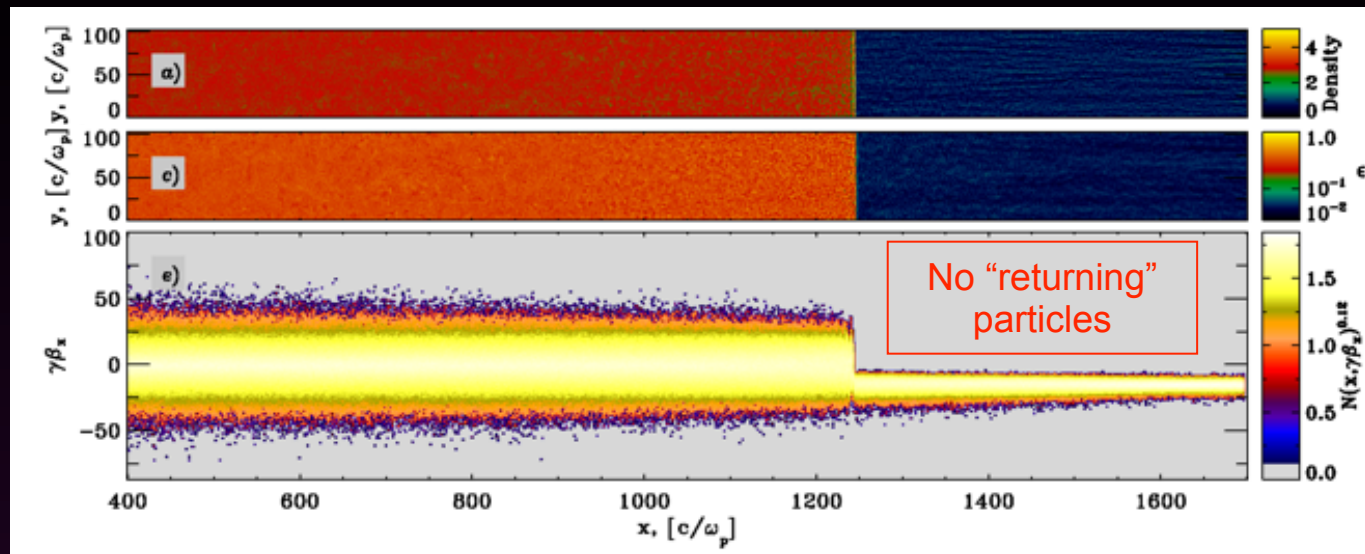
If shocks, then the field is \perp to the shock normal

$$\sigma = \frac{B_0^2}{4\pi\gamma_0 n_0 m_p c^2}$$



Shocks: no turbulence \rightarrow no acceleration

$\sigma=0.1$ $\theta=90^\circ$ $\gamma_0=15$ e⁻-e⁺ shock



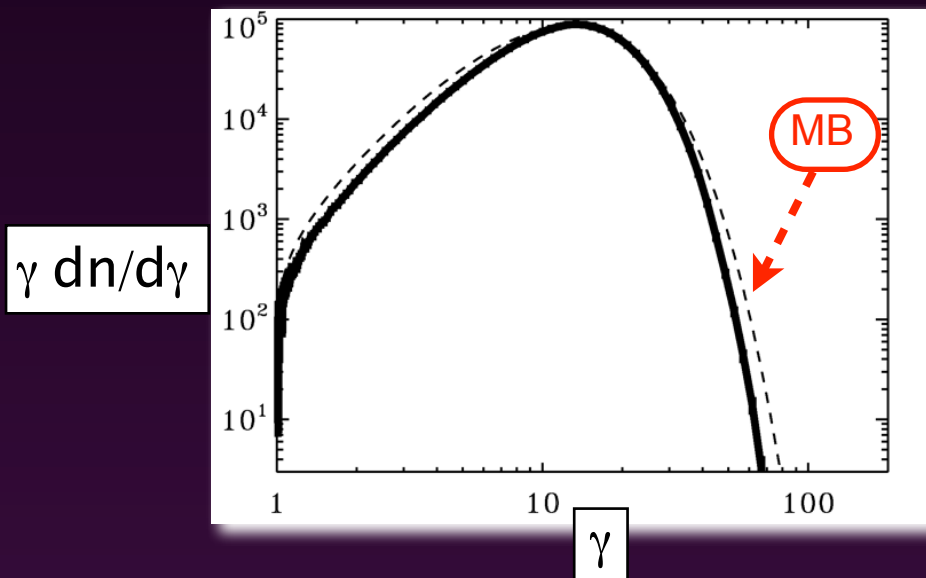
Density

ϵ_B

$\gamma\beta_x$

No "returning" particles \rightarrow No self-generated turbulence

No self-generated turbulence \rightarrow No particle acceleration

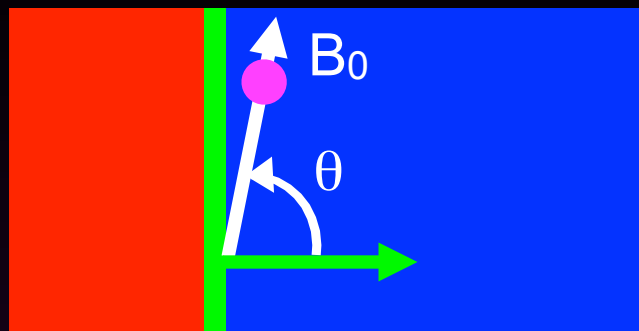


Spectrum fitted by a Maxwellian

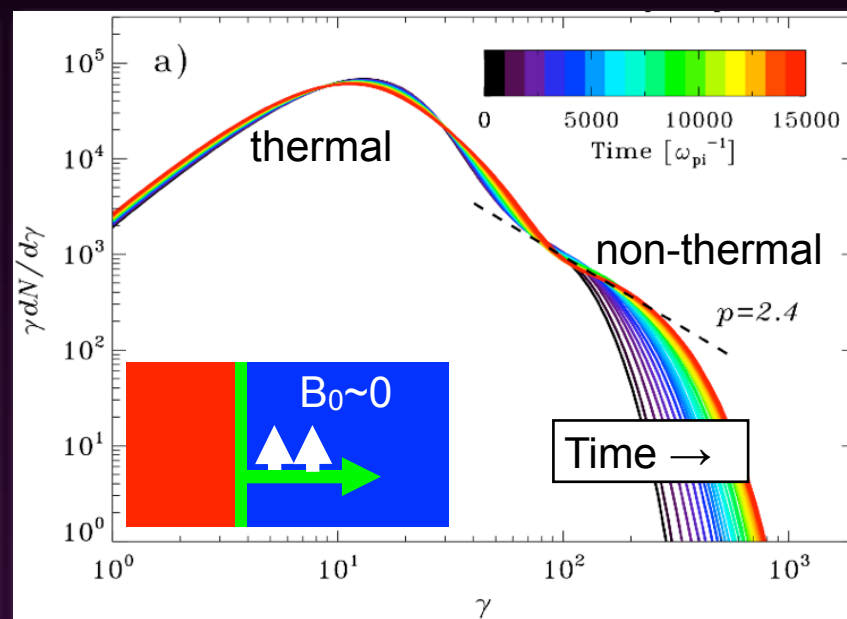
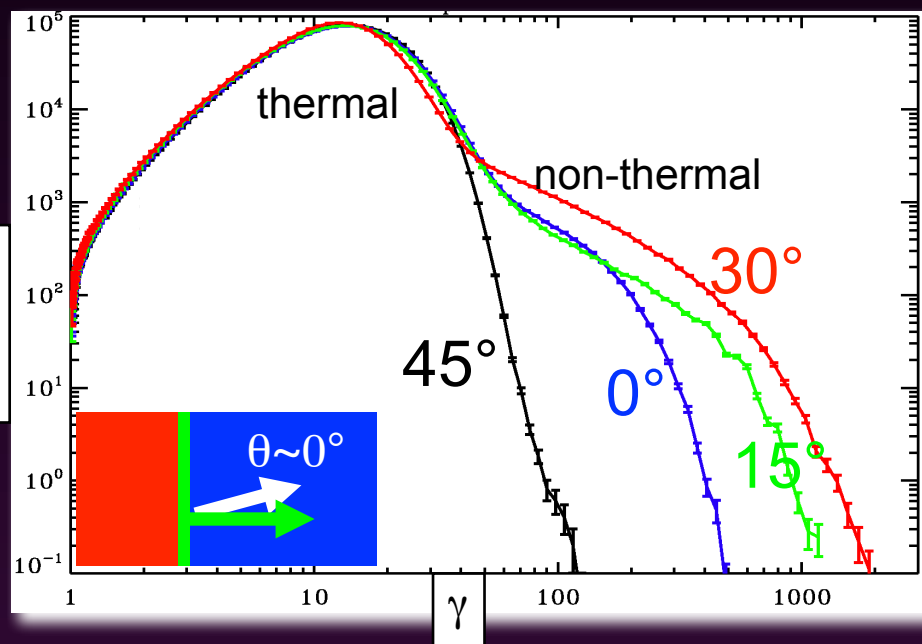
(LS & Spitkovsky 11a)

The shock(ing) puzzle

Strongly magnetized ($\sigma > 10^{-3}$) quasi-perp $\gamma_0 \gg 1$ shocks are poor particle accelerators



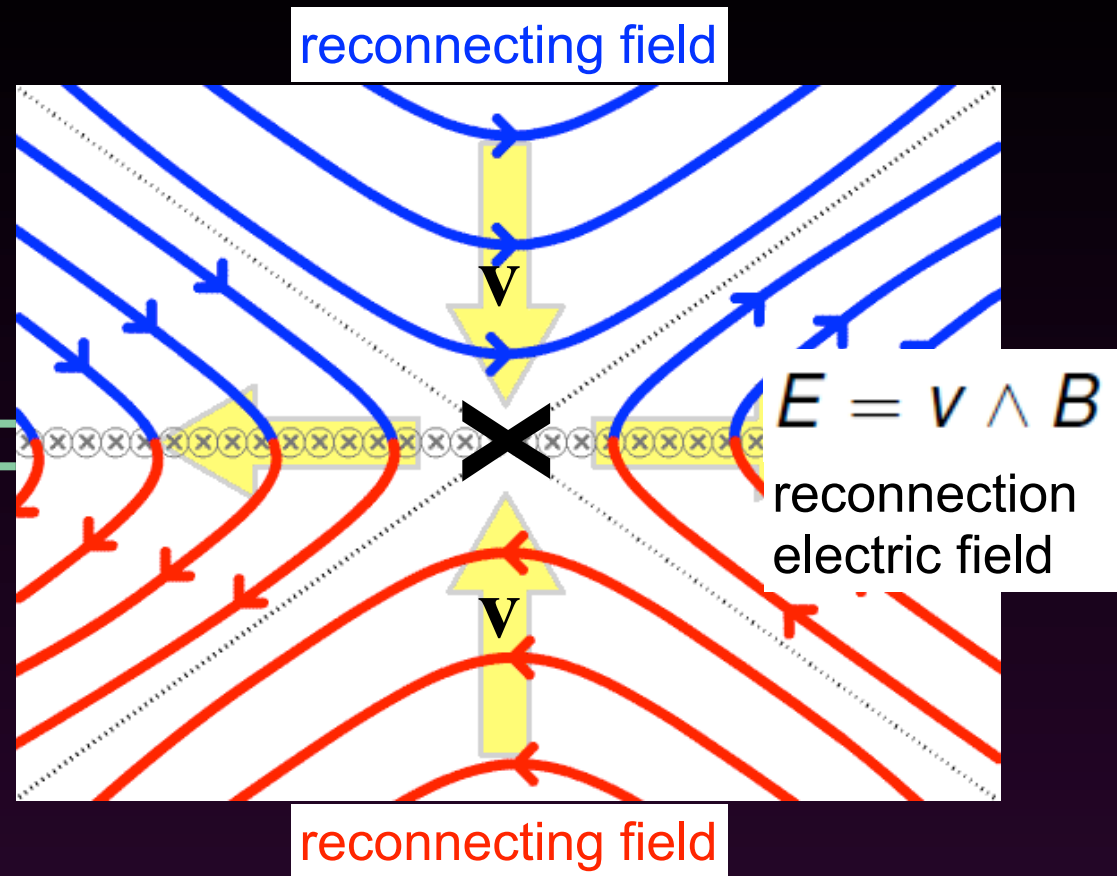
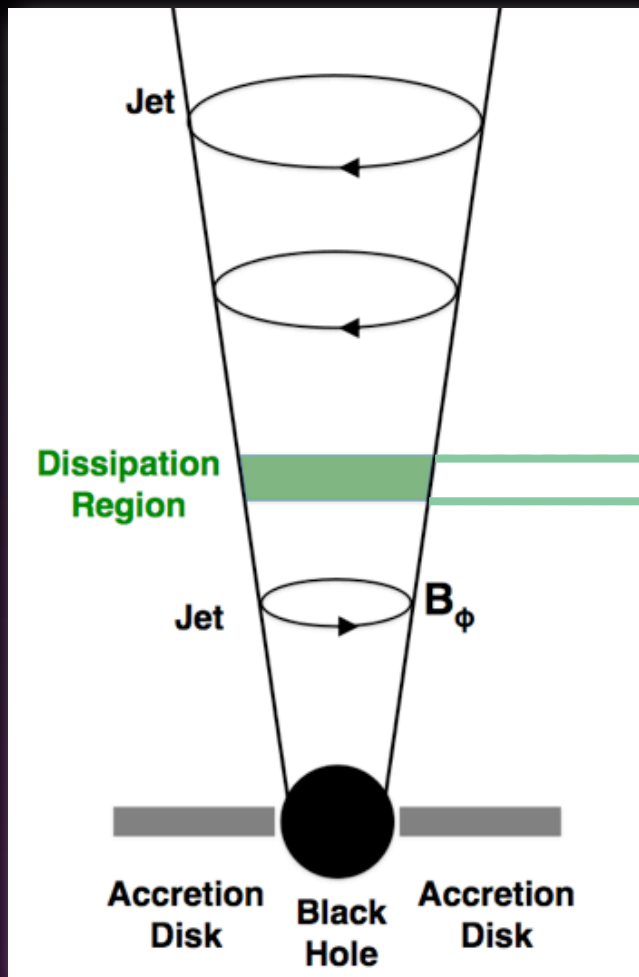
σ is large \rightarrow particles slide along field lines
 θ is large \rightarrow particles cannot outrun the shock
 unless $v > c$ (“superluminal” shock)
 \rightarrow Fermi acceleration is generally suppressed



(LS et al. 13)

- Non-thermal energy spectra from shocks are steep ($p > 2$).
- Shocks are not a natural explanation for the fast time variability.

Relativistic magnetic reconnection



Relativistic Reconnection

$$\sigma = \frac{B_0^2}{4\pi n_0 m_p c^2} \gg 1$$

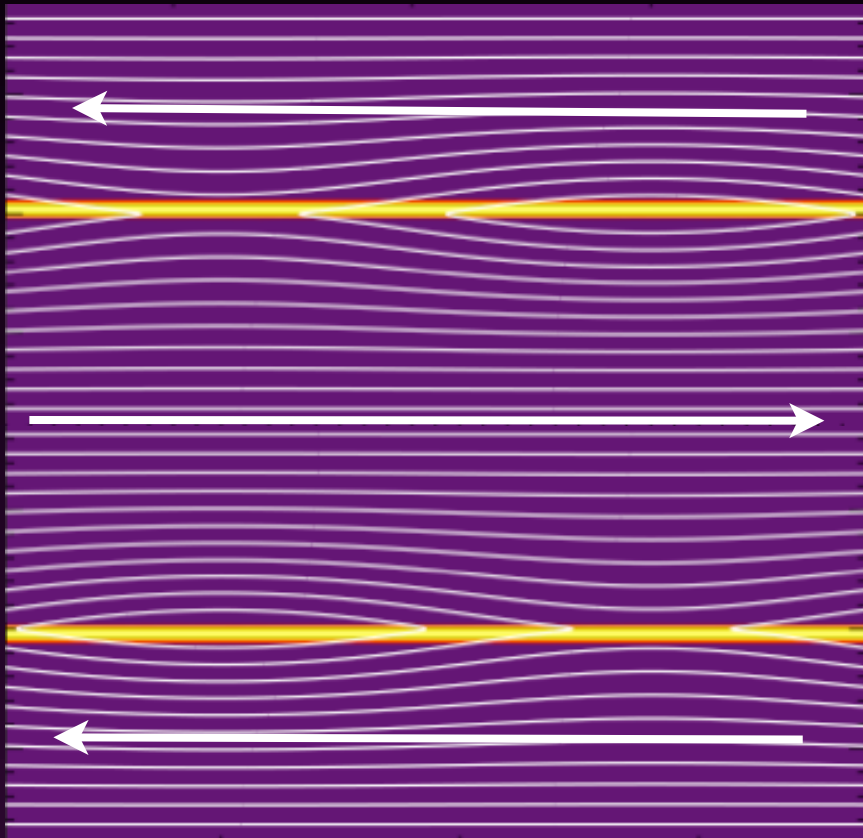
References: most of the people in this room

Can relativistic magnetic reconnection self-consistently produce non-thermal particles?

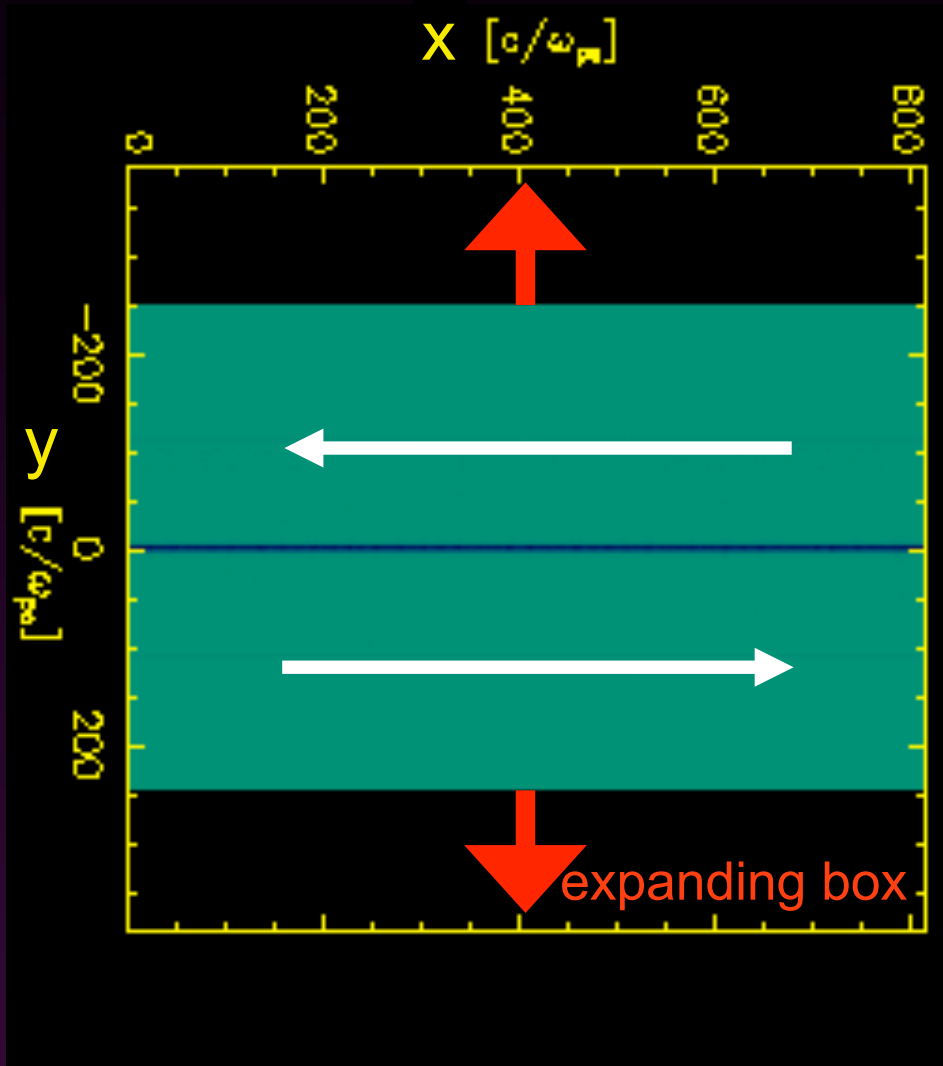
Simulation setup

Relativistic 3D e.m. PIC code TRISTAN-MP (Buneman '93, Spitkovsky '05)

What is the long-term evolution of relativistic magnetic reconnection?



double-periodic boundary conditions

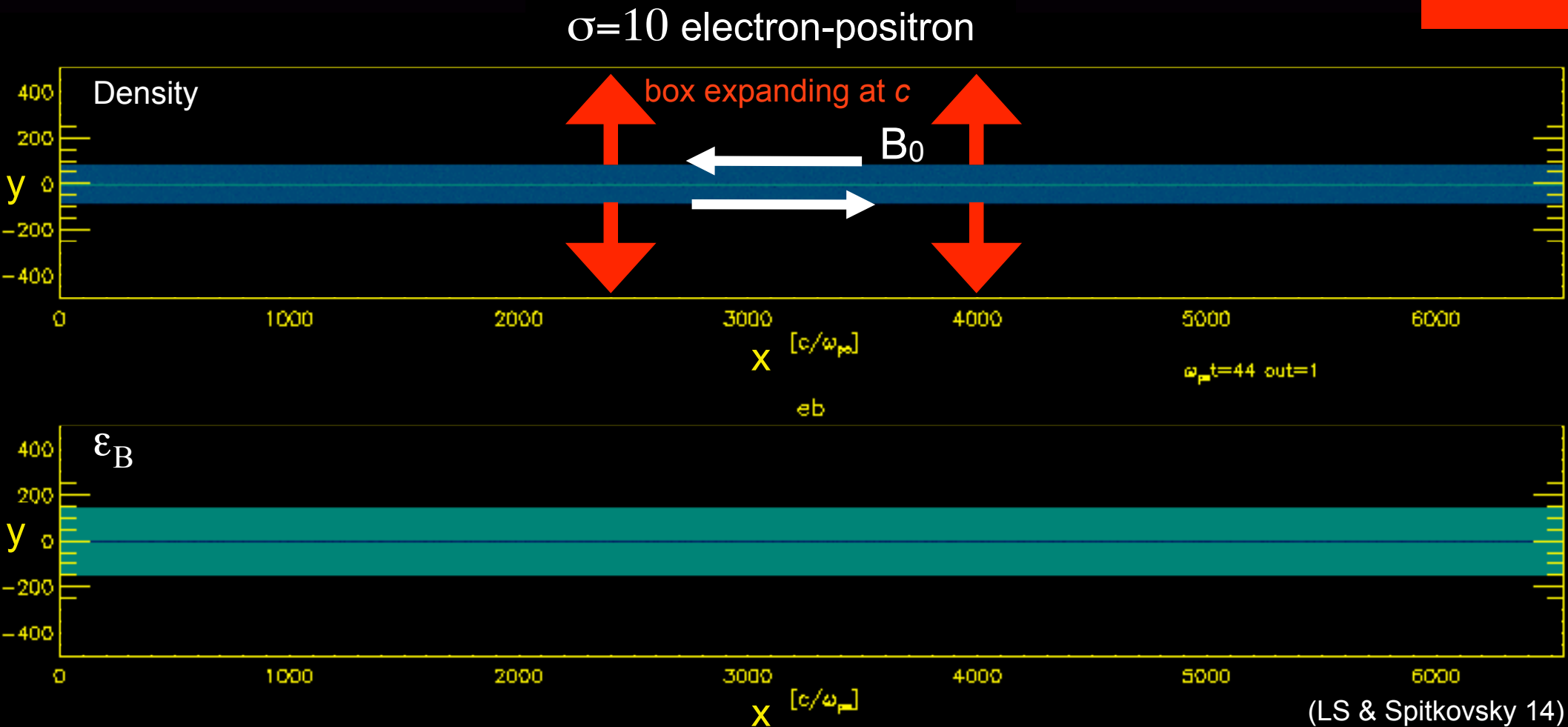


periodic in x, expanding along y at c



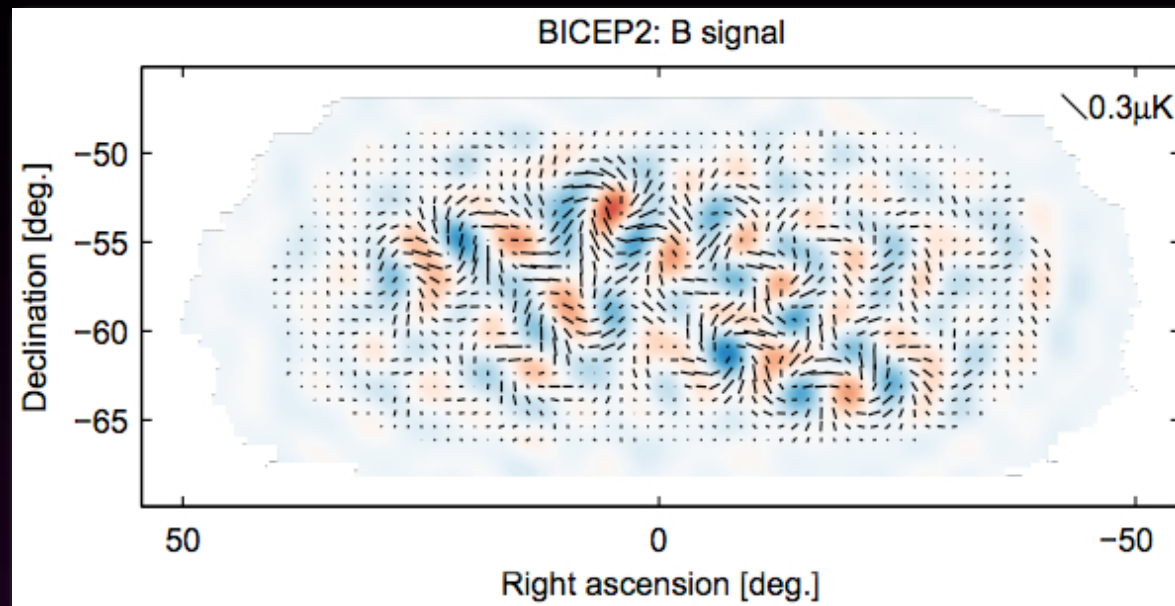
Dynamics and particle spectrum

Hierarchical reconnection

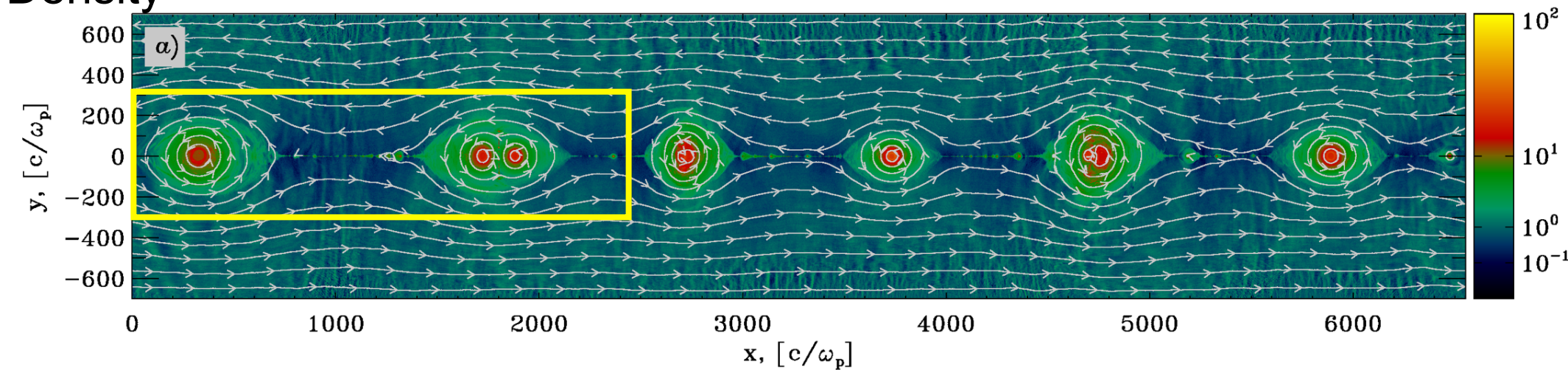


- Reconnection is a hierarchical process of island formation and merging.
- The field energy is transferred to the particles at the X-points, in between the magnetic islands.

Structure of the reconnection layer



Density

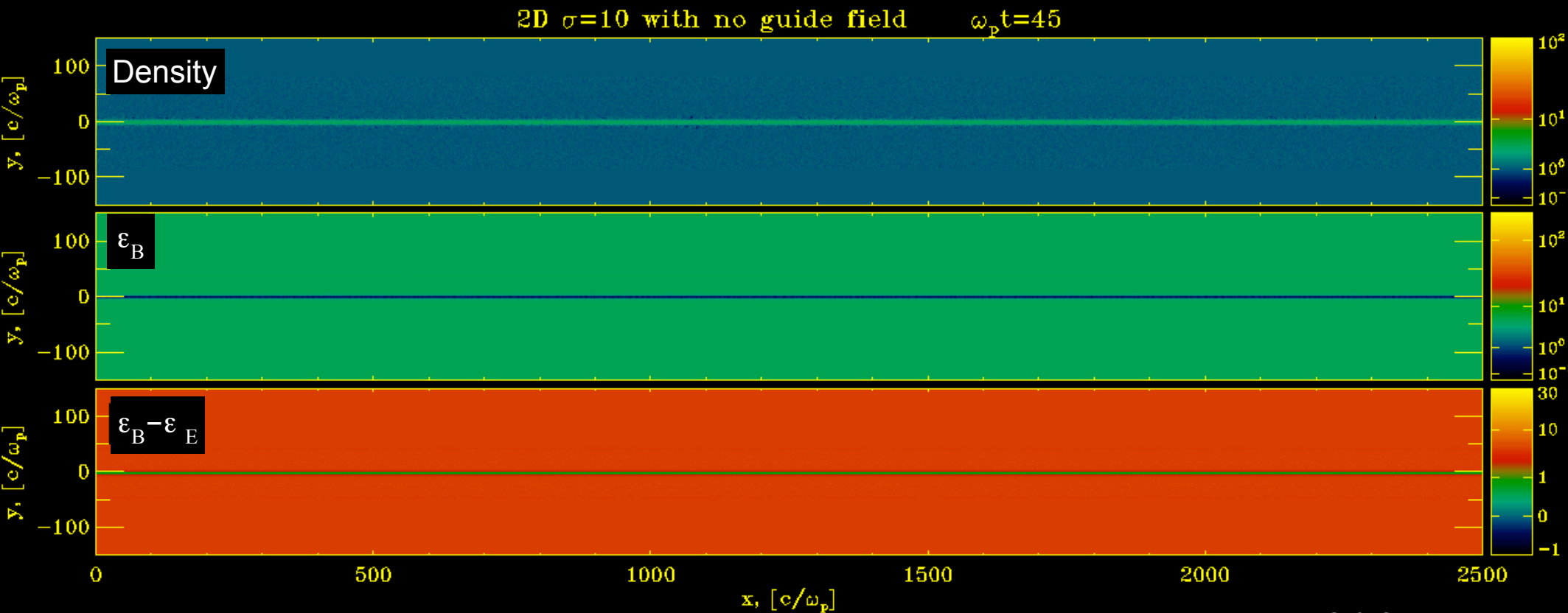
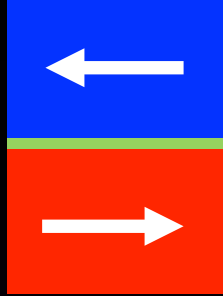


Reconnection rate: $r = \frac{v_{in}}{v_A}$

$v_A = c \sqrt{\frac{\sigma}{1 + \sigma}} \sim c$

Hierarchical reconnection

$\sigma=10$ electron-positron

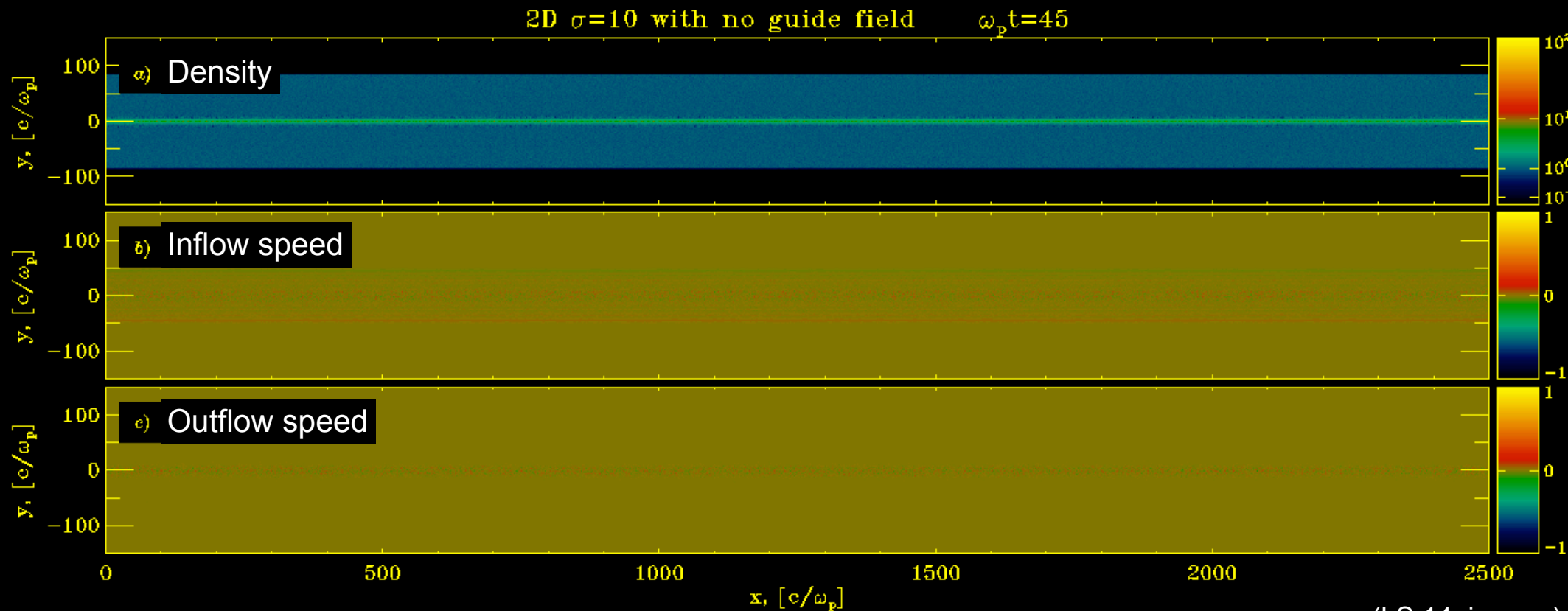
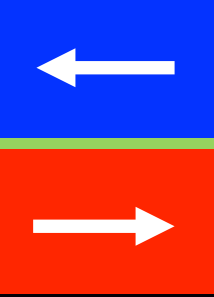


(LS & Spitkovsky 14)

- Reconnection is a hierarchical process of island formation and merging.
- The field energy is transferred to the particles at the X-points, in between the magnetic islands.
- Anti-reconnection occurs at the interface between two merging islands.

Inflows and outflows

$\sigma=10$ electron-positron

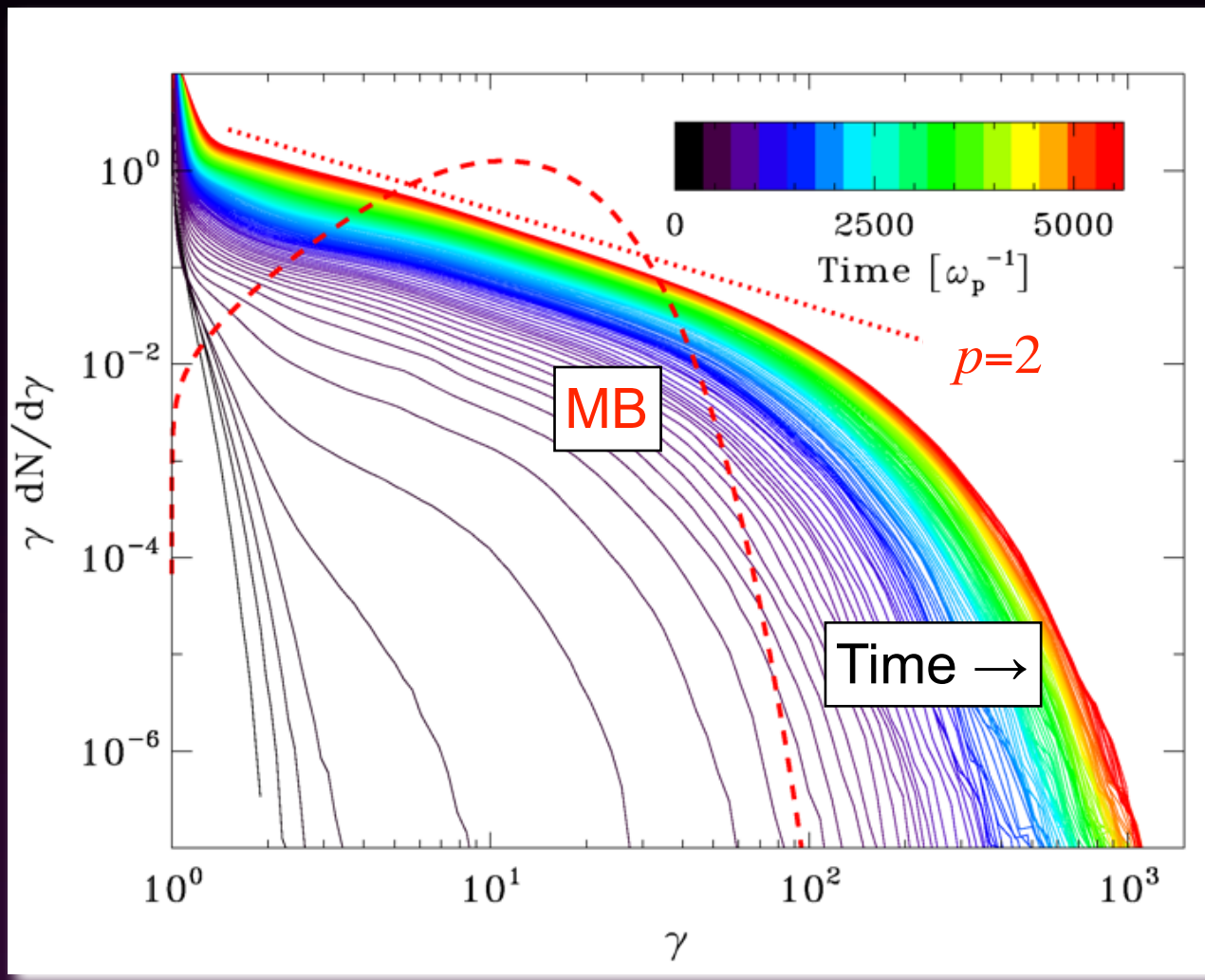


(LS 14, in prep)

- Inflow into the X-line is non-relativistic, $v_{\text{in}} \sim 0.1 c$ (so, the reconnection rate $r \sim 0.1$).
- Outflow into the islands is ultra-relativistic, at the Alfvén speed $v_A = c \sqrt{\frac{\sigma}{1 + \sigma}}$

The particle energy spectrum

$\sigma=10$ electron-positron



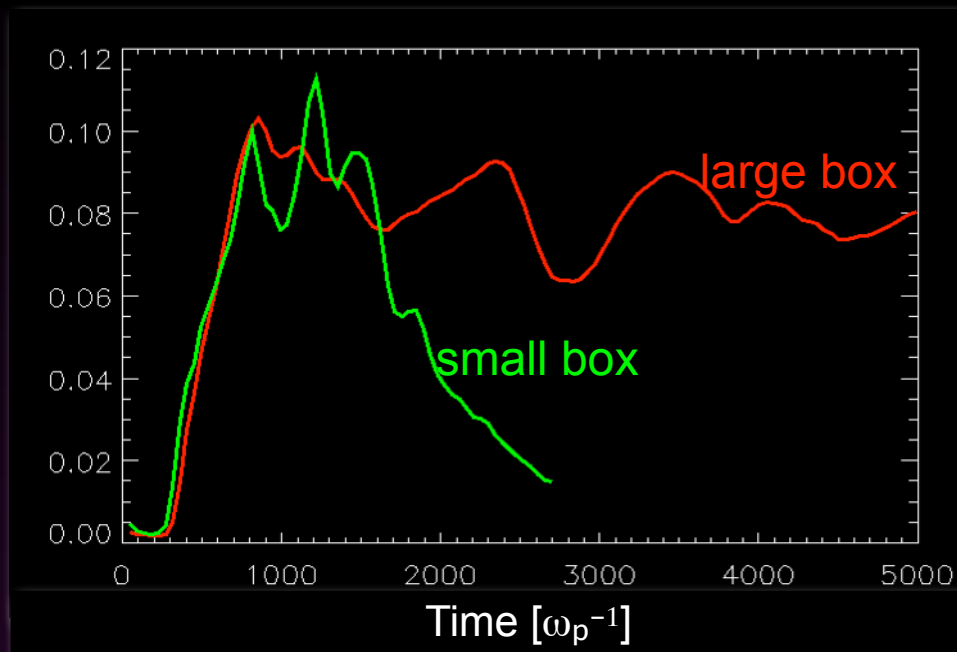
(LS & Spitkovsky 14)

- At late times, the particle spectrum in the current sheet approaches a power-law tail $dn/d\gamma \propto \gamma^{-p}$ of slope $p \sim 2$.
- The normalization increases, as more and more particles enter the current sheet.
- The mean particle energy in the current sheet is $\sim \sigma/2$
→ energy equipartition

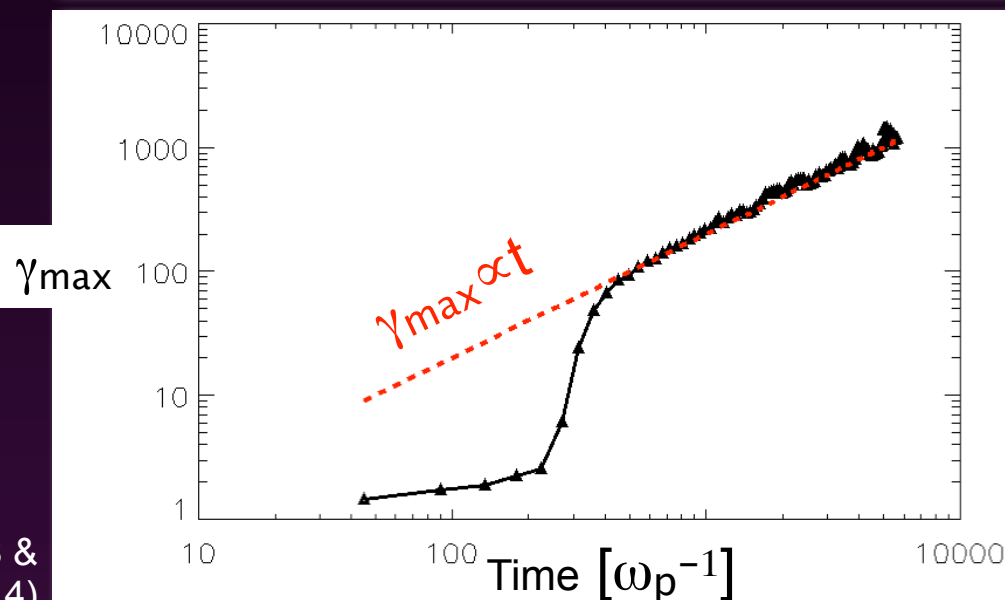
The maximum particle energy

$\sigma=10$ electron-positron

$$r \sim v_{\text{in}}/c$$



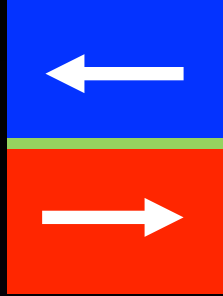
- The reconnection rate r stays nearly constant in time, if the evolution is not artificially inhibited by the boundaries.



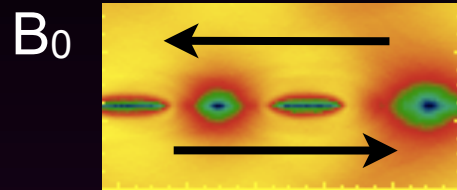
(LS & Spitkovsky 14)

- The maximum energy grows at a rate $\sim r$ so that $\gamma_{\text{max}} \propto t$ (compare to $\gamma_{\text{max}} \propto t^{1/2}$ in relativistic shocks).

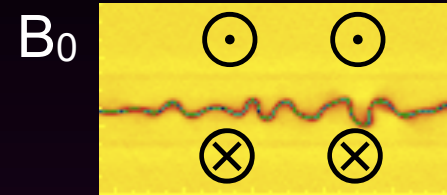
Tearing mode vs drift-kink mode



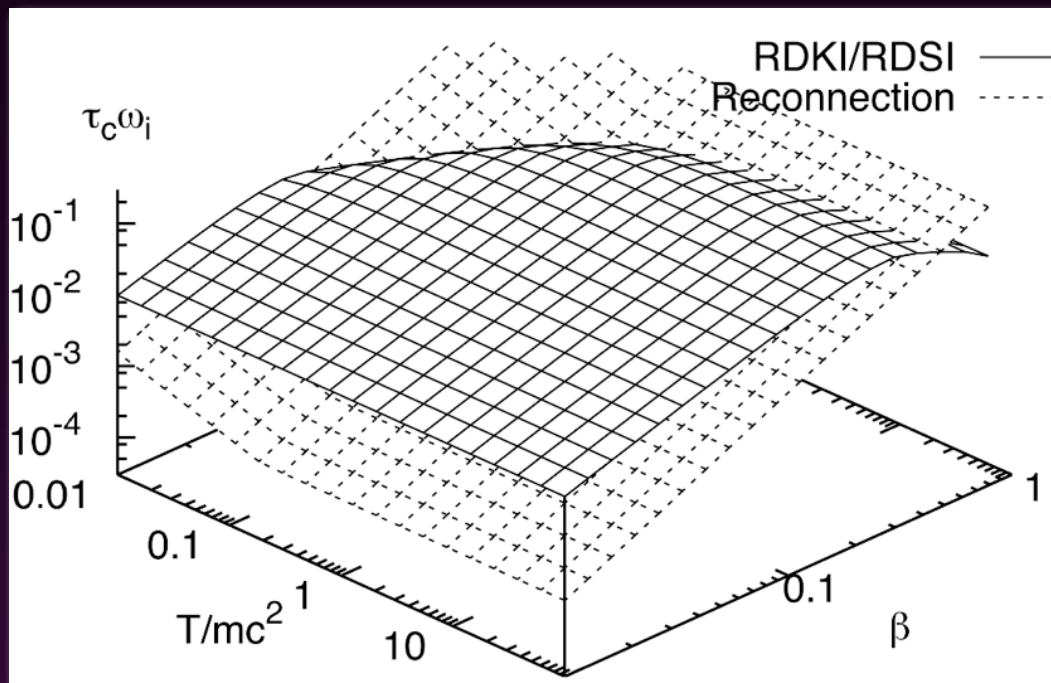
TEARING mode in the plane of alternating fields



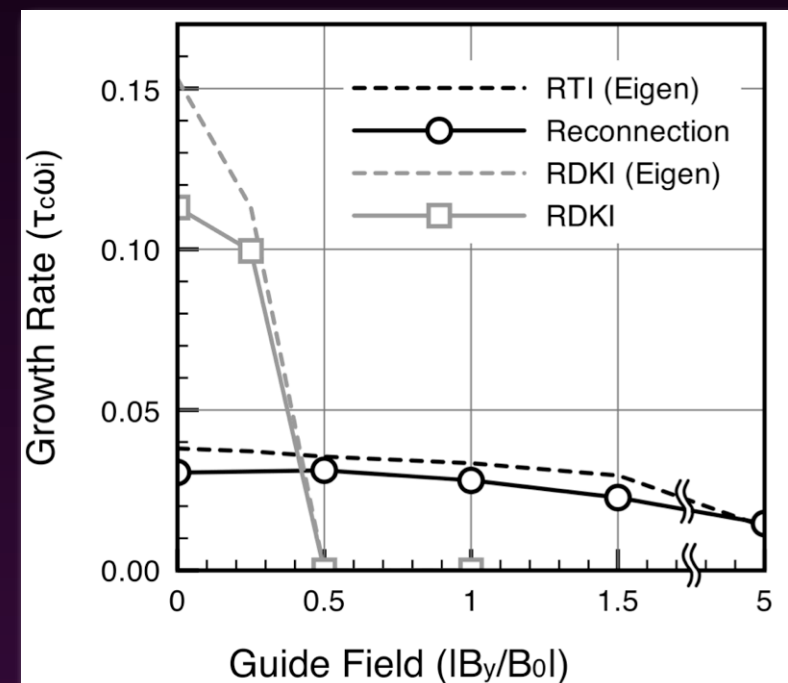
DRIFT-KINK mode perp to the plane of alternating fields



Which mode dominates in 3D?

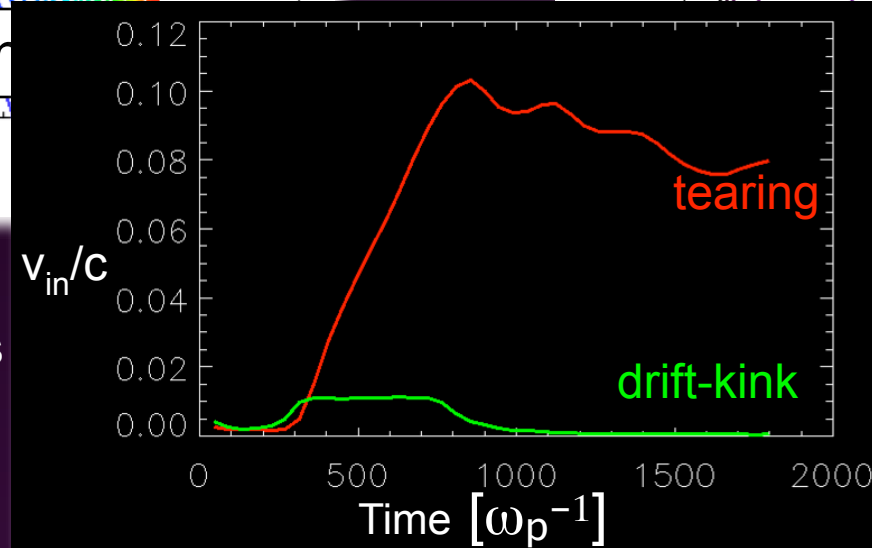
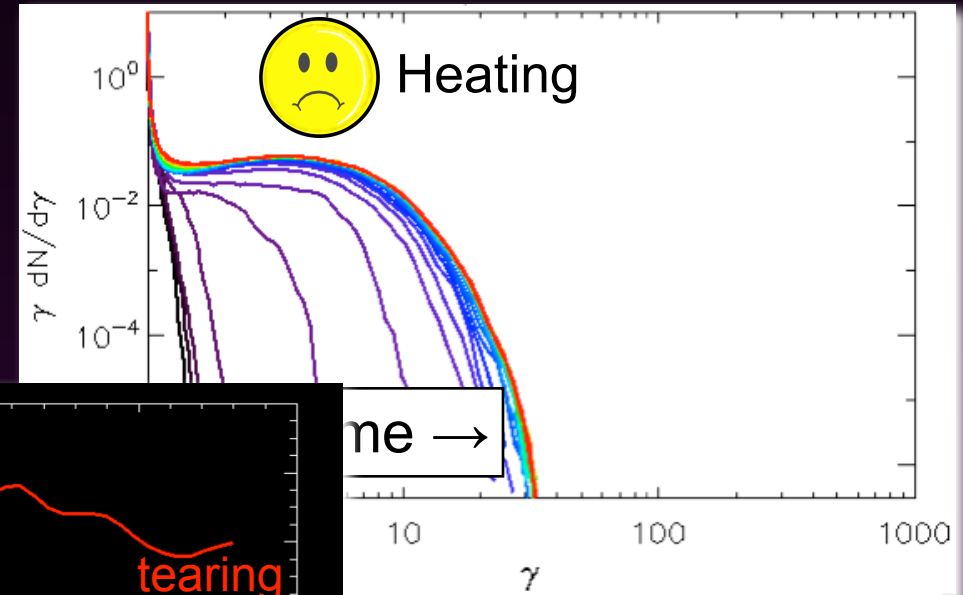
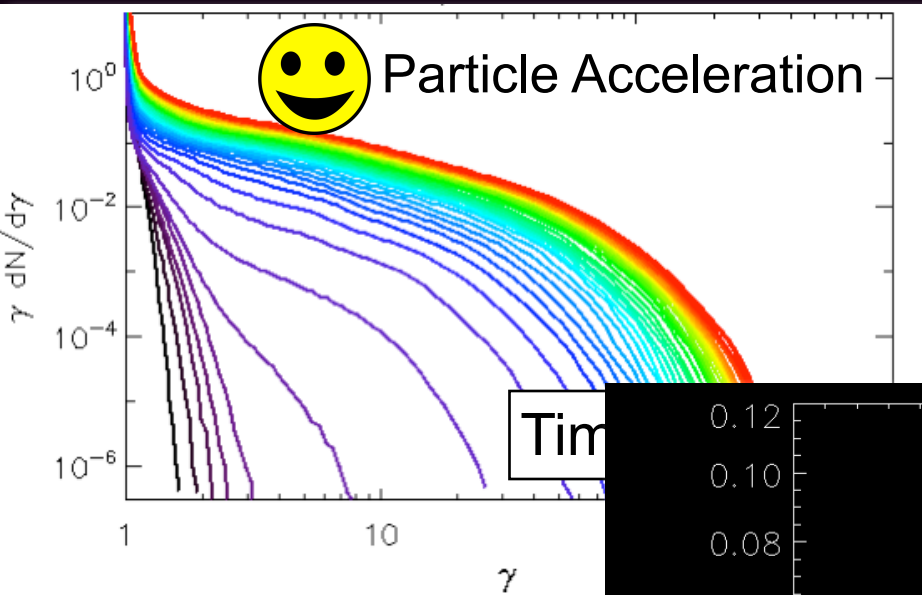
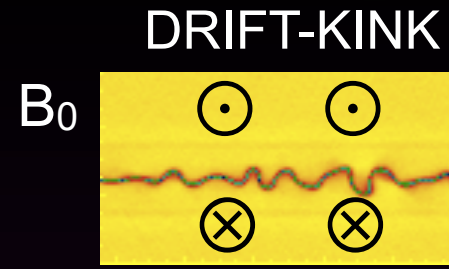
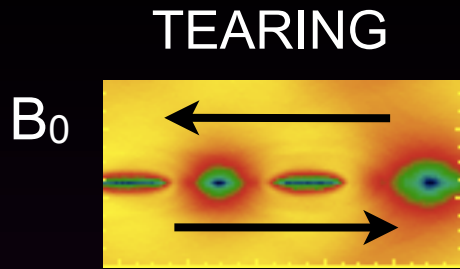


(Zenitani & Hoshino 07)



(Zenitani & Hoshino 08)

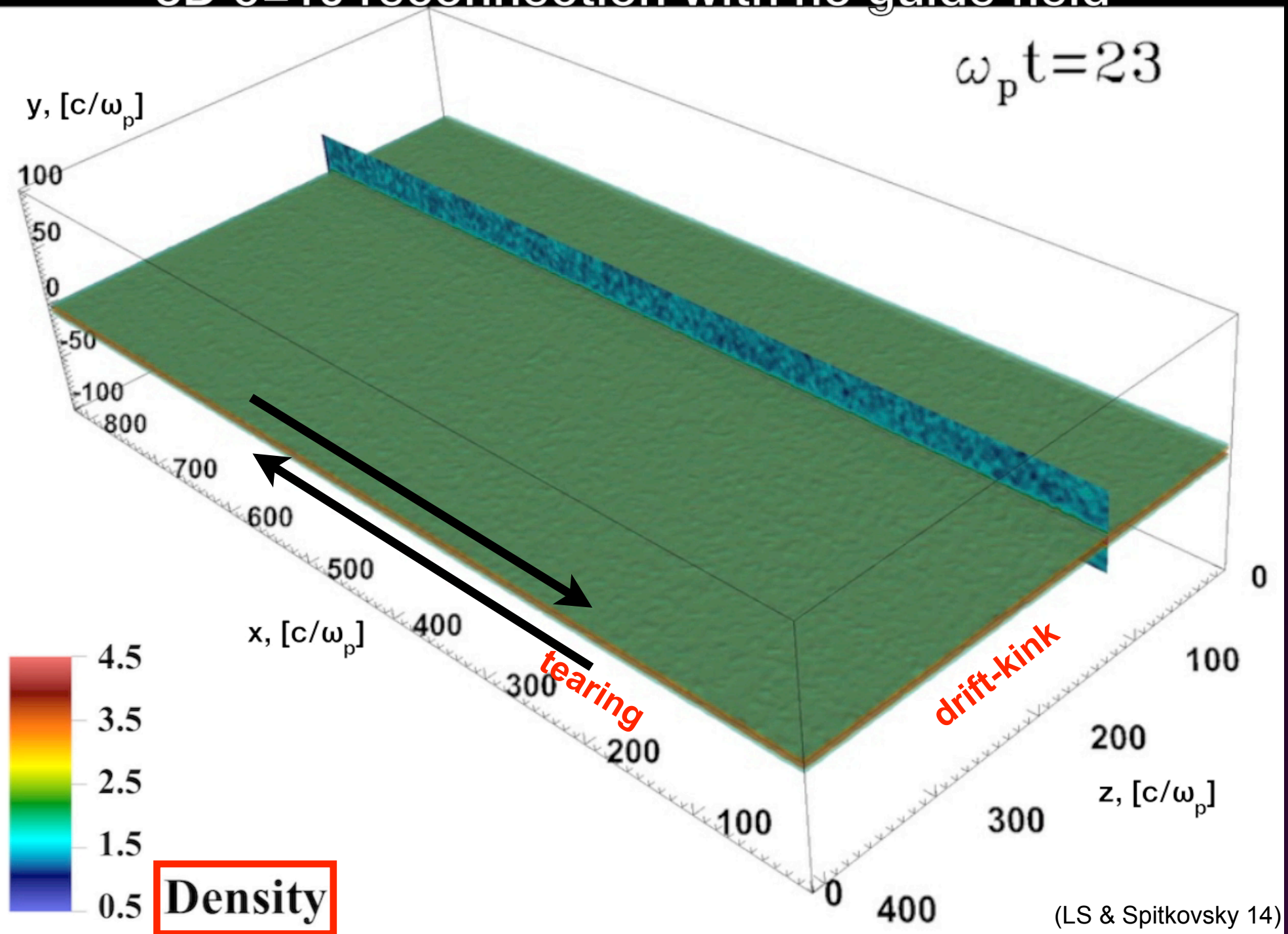
Particle acceleration vs heating



The DK mode saturates by broadening the current sheet.

(sop, 600 BC)

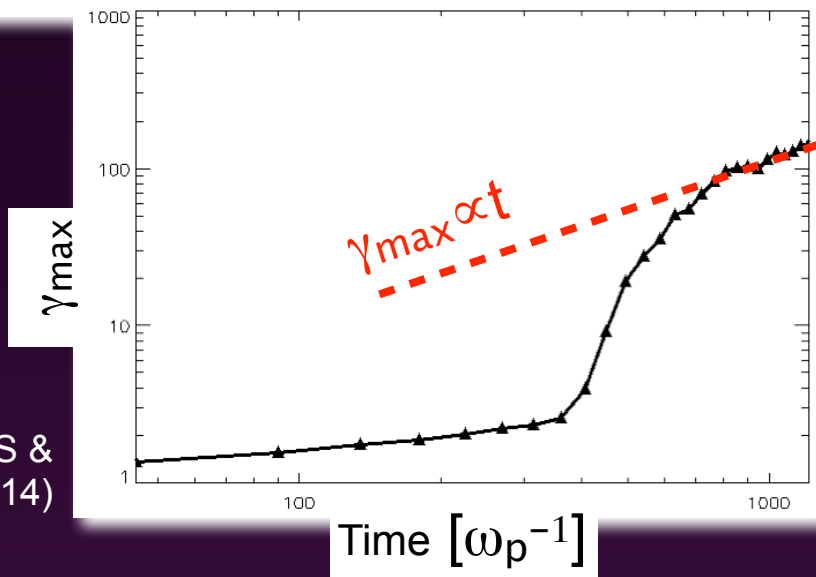
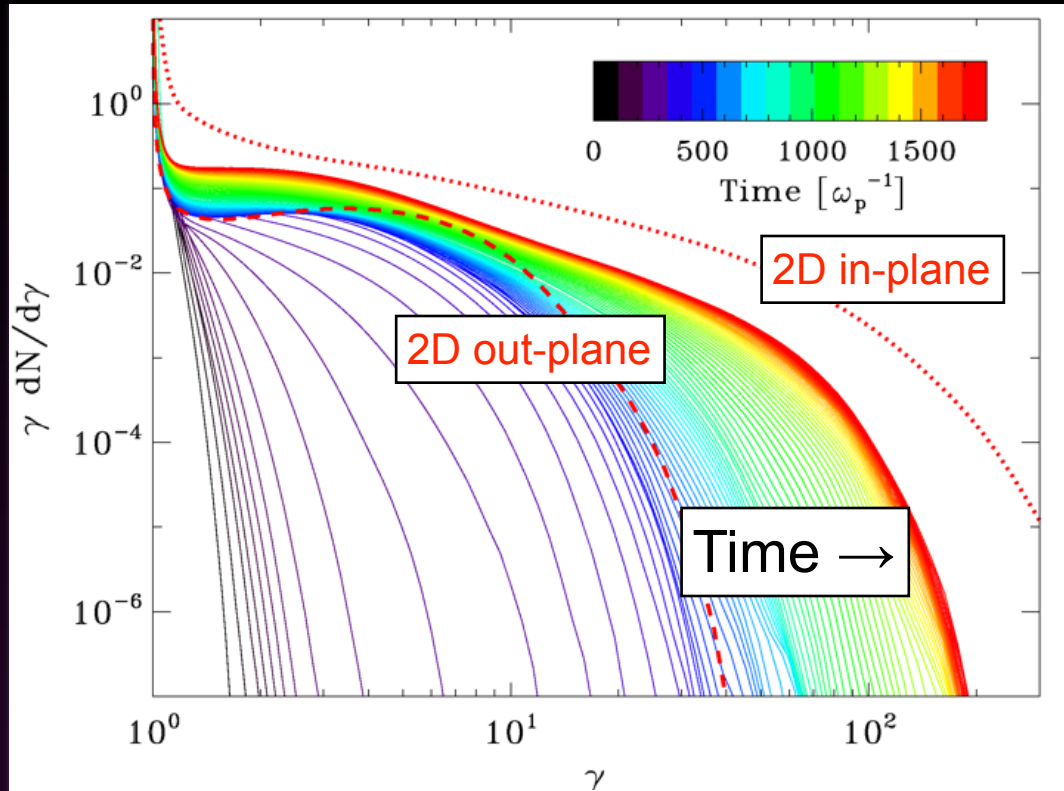
3D $\sigma=10$ reconnection with no guide field



In 3D, the in-plane tearing mode controls the evolution at late times.

3D: particle spectrum

$\sigma=10$ electron-positron



(LS & Spitkovsky 14)

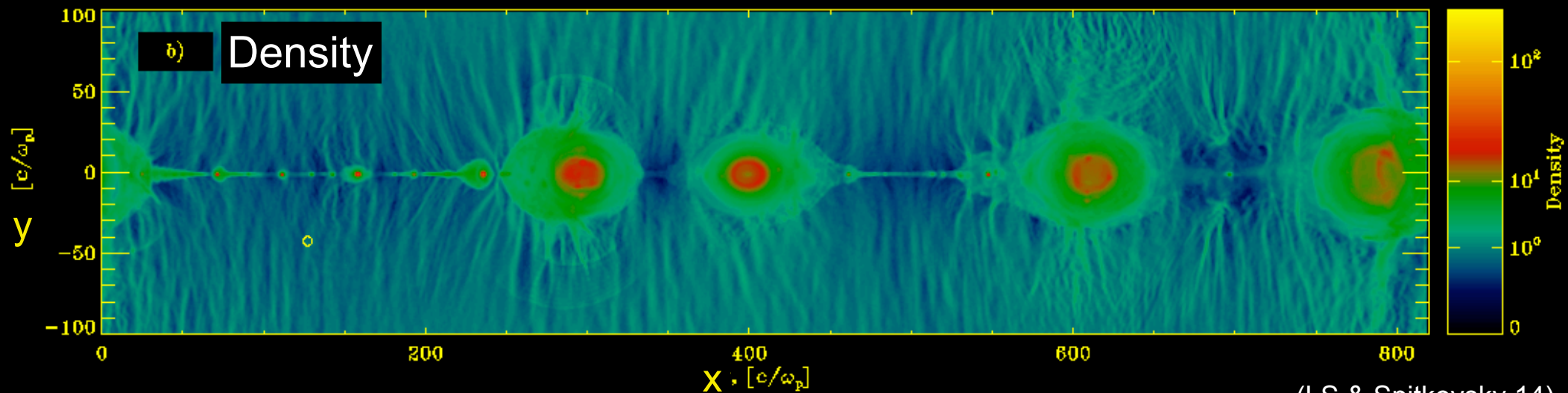
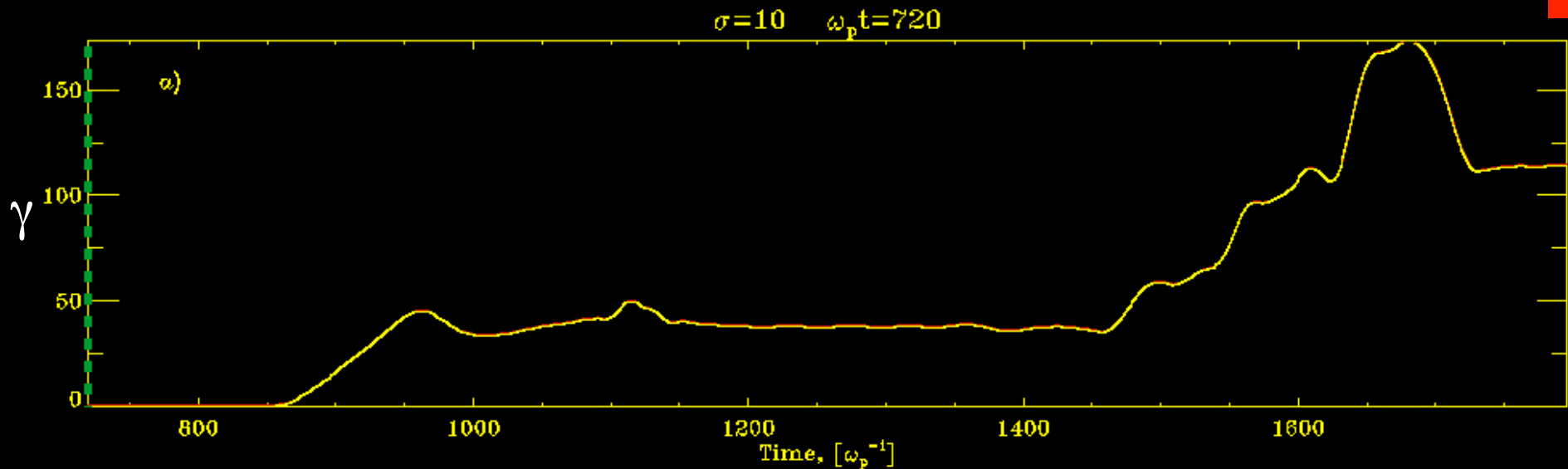
- At late times, the particle spectrum approaches a power-law tail of slope $p \sim 2$, extending in time to higher and higher energies. The same as in 2D.

- The maximum energy grows as $\gamma_{\max} \propto t$ (compare to $\gamma_{\max} \propto t^{1/2}$ in shocks). The reconnection rate is $r \sim 0.02$ in 3D (vs $r \sim 0.1$ in 2D).



The acceleration mechanism

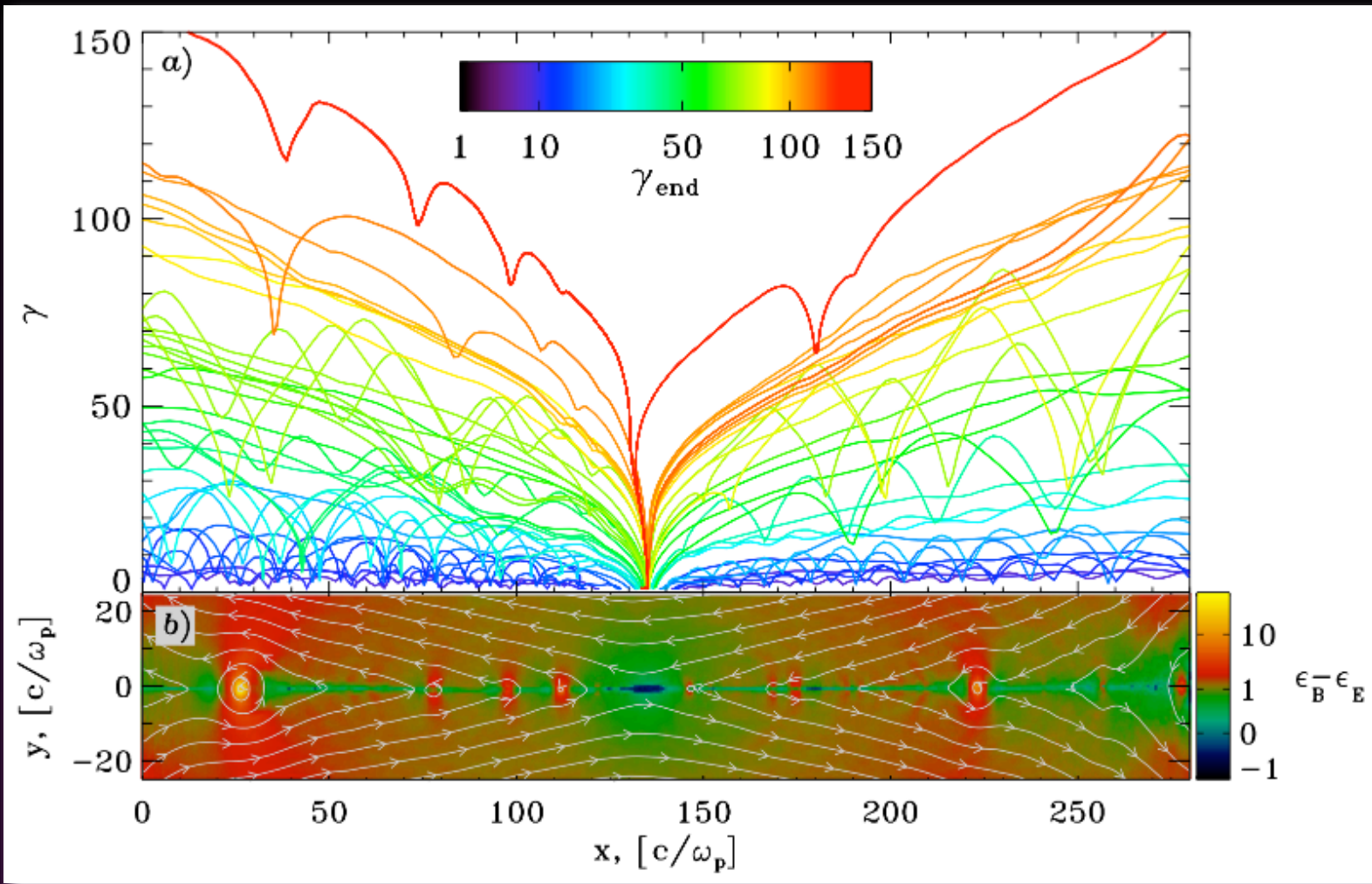
The highest energy particles



(LS & Spitkovsky 14)

Two acceleration phases: 1) at the X-point; 2) in between merging islands

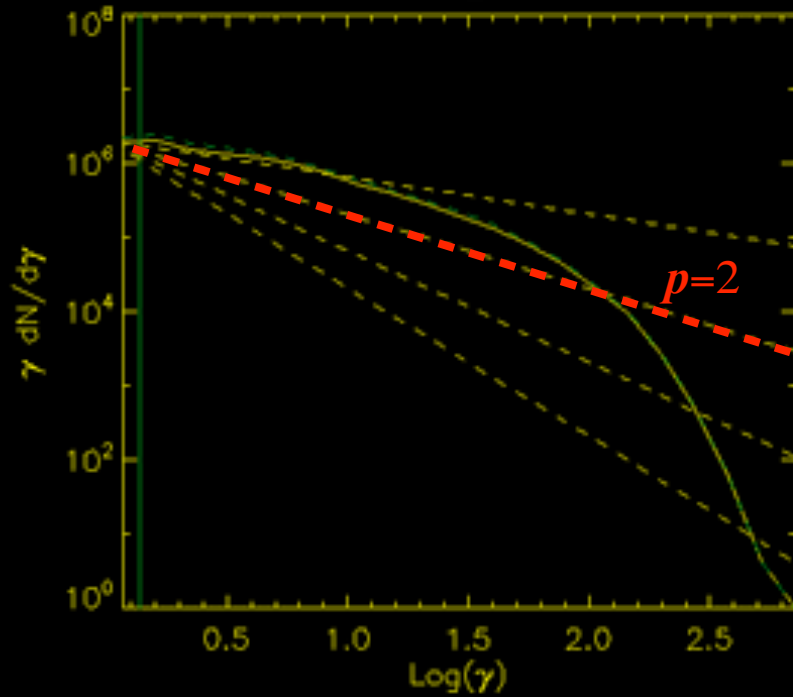
Acceleration at X-points



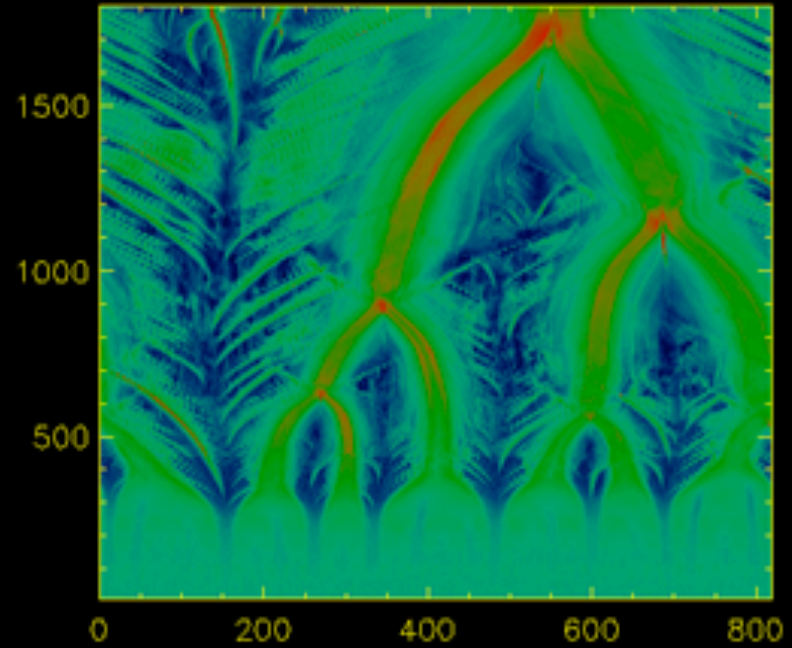
(LS & Spitkovsky 14)

- The particles are accelerated by the reconnection electric field at the X-points, and then advected into the nearest magnetic island.
- The energy gain can vary, depending on where the particle interacts with the sheet.

Primary & secondary X-points

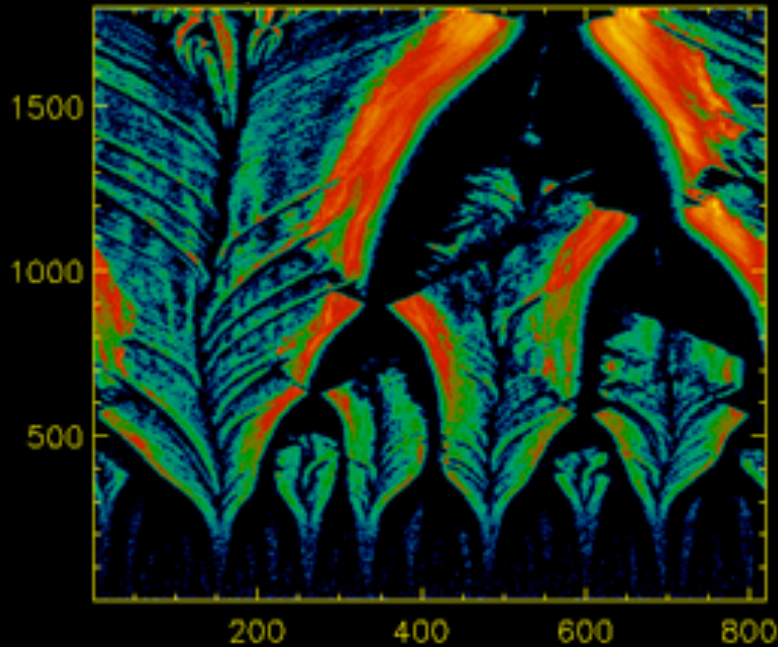


Time [ω_p^{-1}]



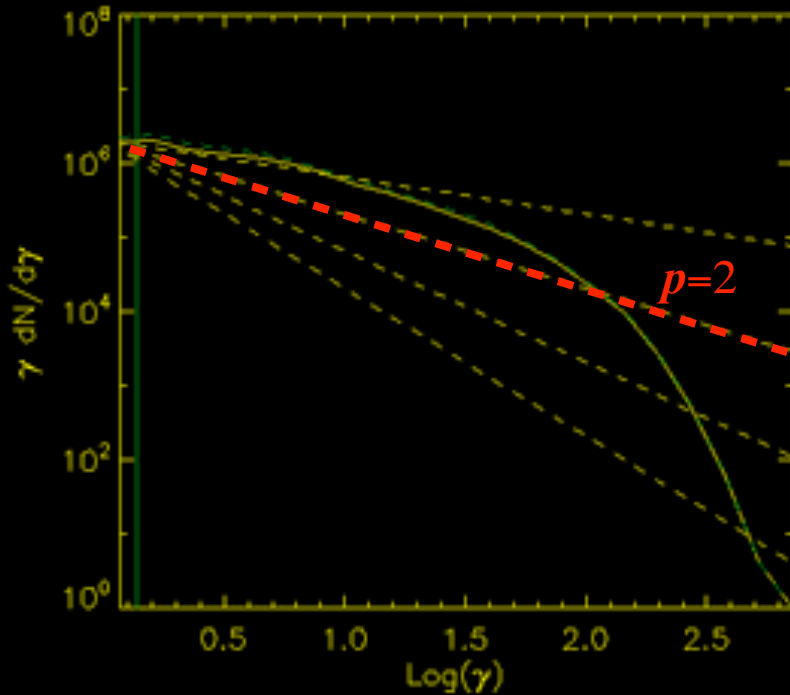
Position along the current sheet [c/ω_p]

Interaction time [ω_p^{-1}]

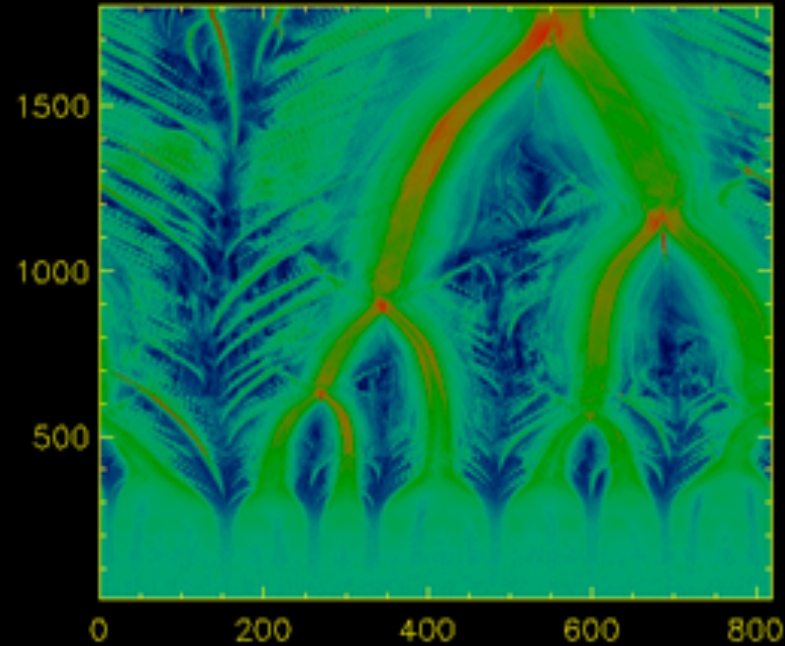


Location at interaction with the current sheet [c/ω_p]

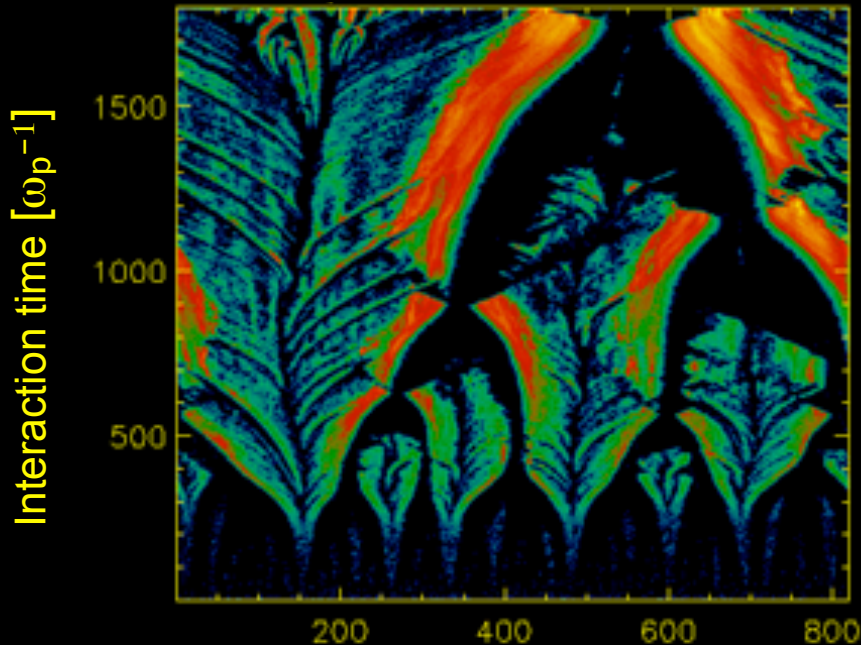
Primary & secondary X-points



Time [ω_p^{-1}]



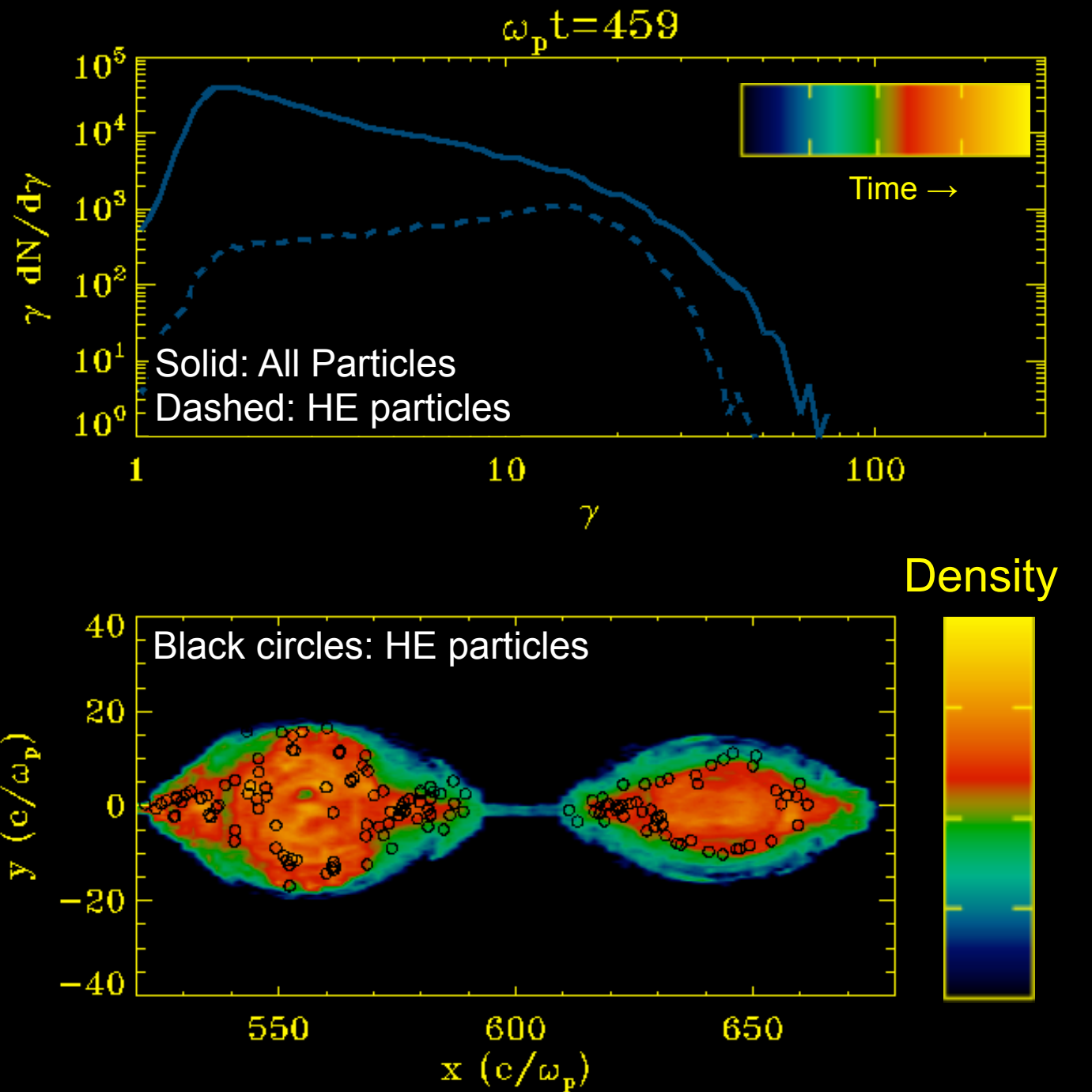
Position along the current sheet [c/ω_p]



Location at interaction with the current sheet [c/ω_p]

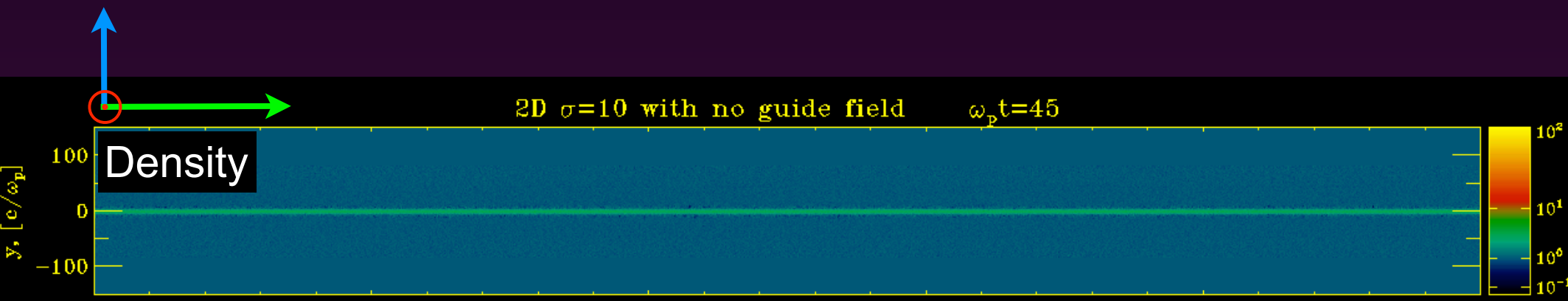
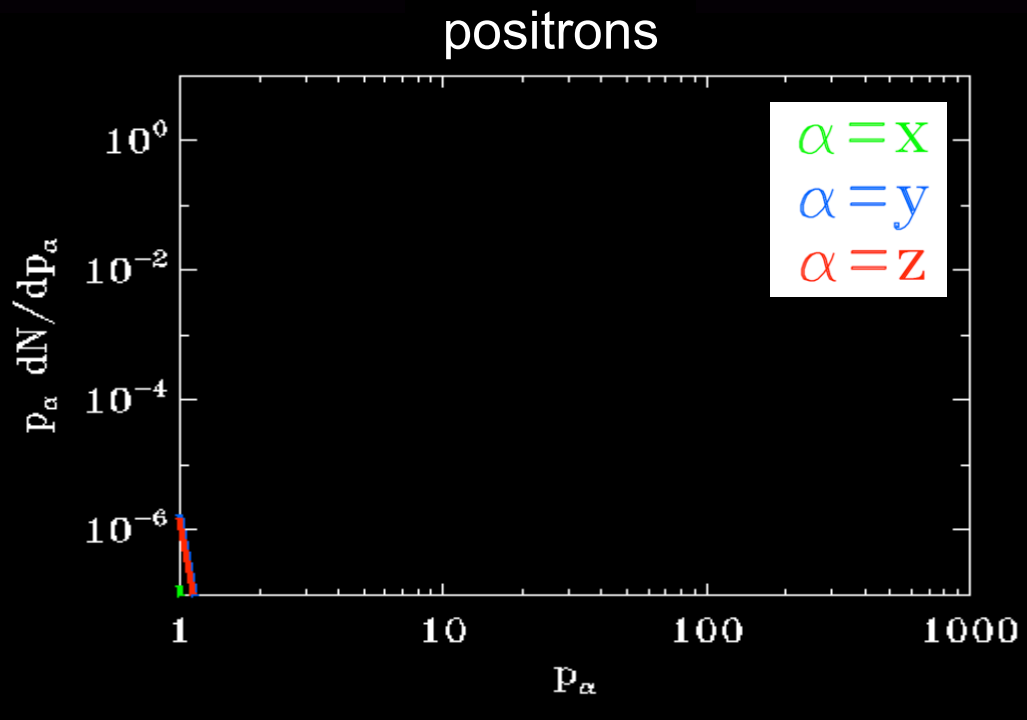
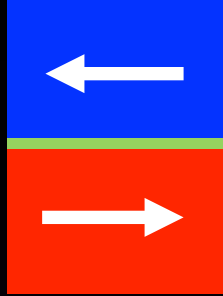
- High-energy particles start their acceleration at both primary and secondary X-points.
- The highest energy particles are injected in a small fraction of the volume.

Fermi acceleration in between islands

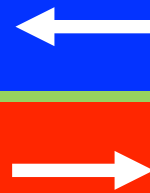


- The particles are accelerated by a Fermi-like process in between merging islands.
- Island merging is essential to shift up the spectral cutoff energy.

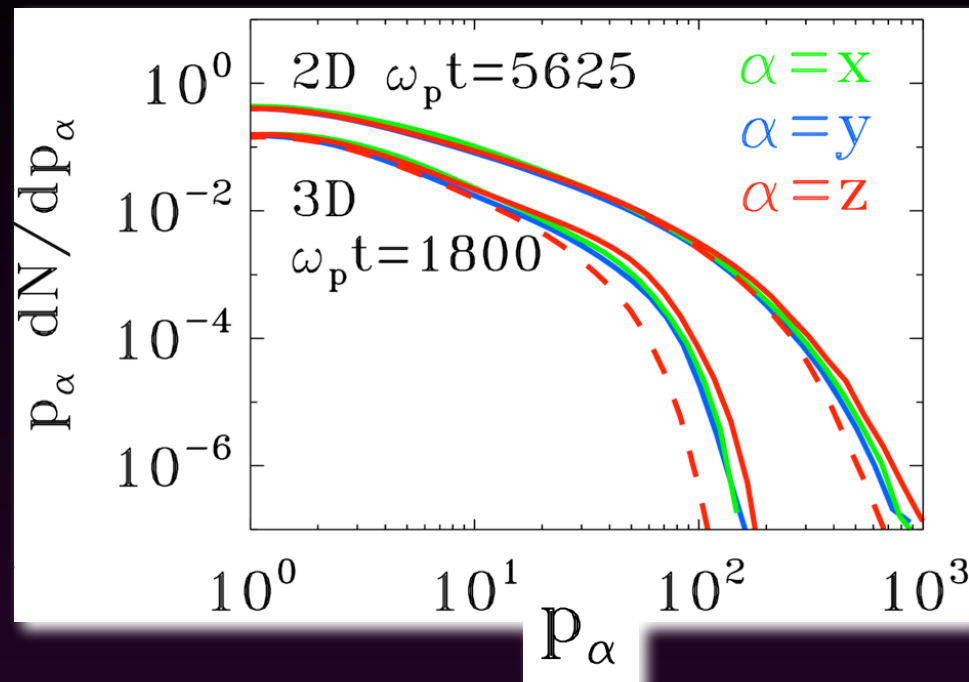
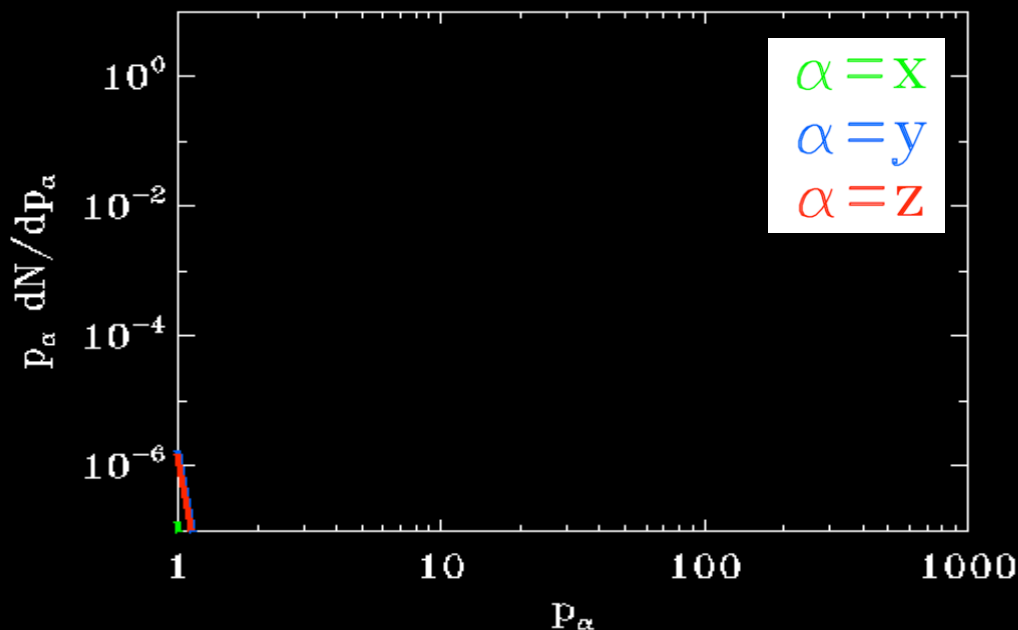
Anisotropy of the accelerated particles



Anisotropy of the accelerated particles

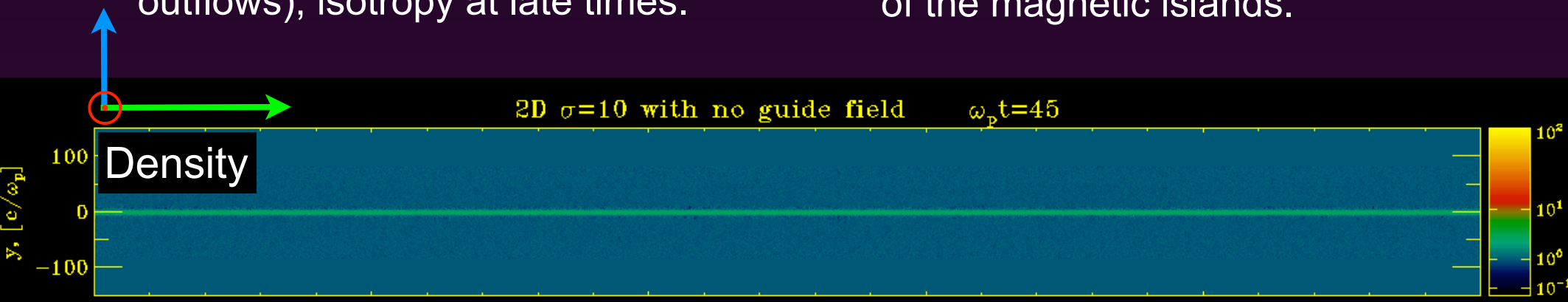


positrons



Anisotropy at early times (first along the reconnection E field, and then along the outflows), isotropy at late times.

The residual anisotropy at late times comes from ∇B drift in the outskirts of the magnetic islands.

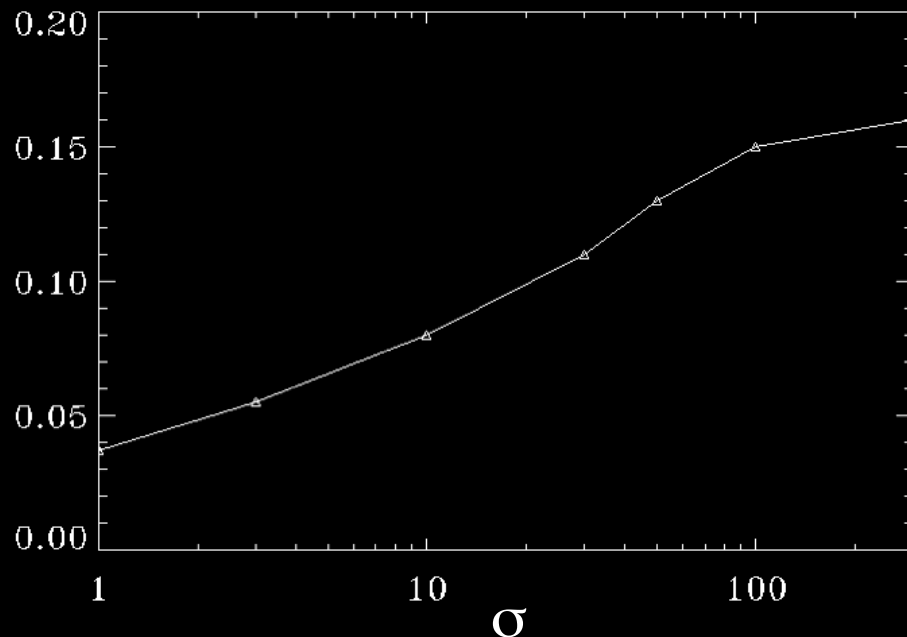


Dependence on the flow conditions

Dependence on the magnetization

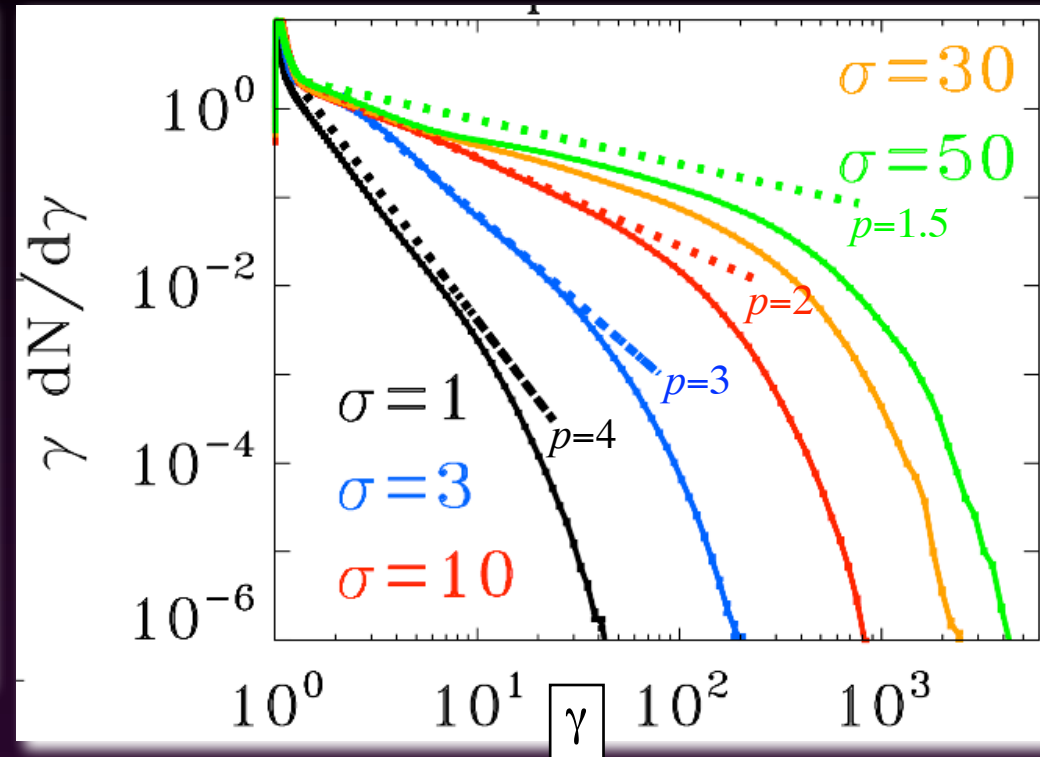
$$\sigma = \frac{B_0^2}{4\pi n_0 m_p c^2}$$

v_{in}/c



As σ increases:

- the reconnection rate saturates at $\sim 0.15 c$



(LS 14, in prep)

As σ increases:

- the power-law slope becomes harder
 \Rightarrow a probe of the flow magnetization?

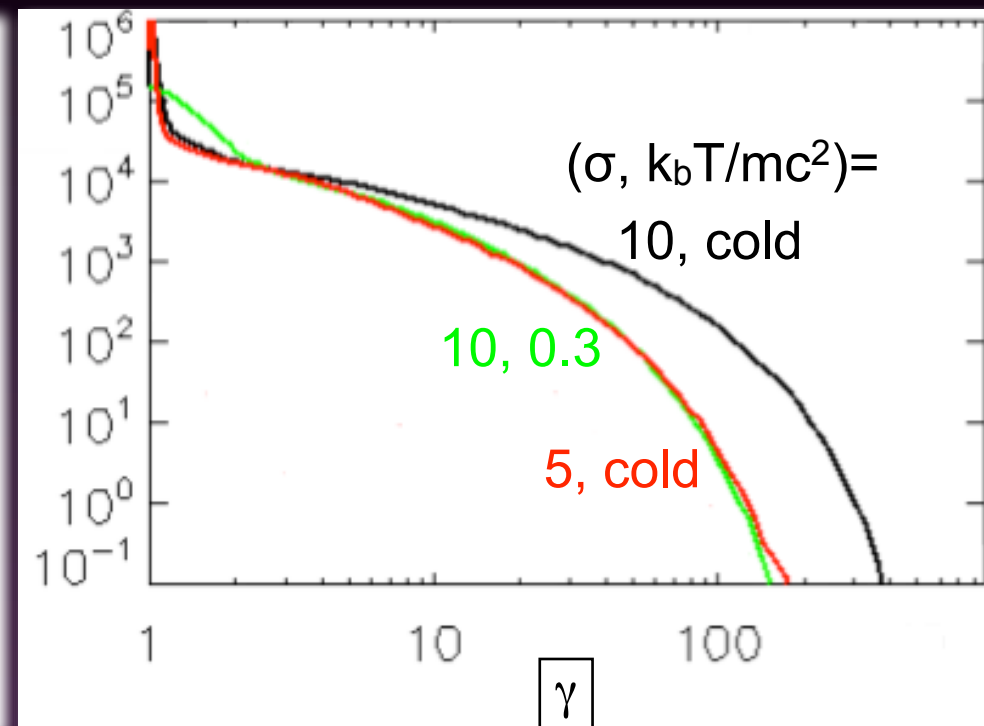
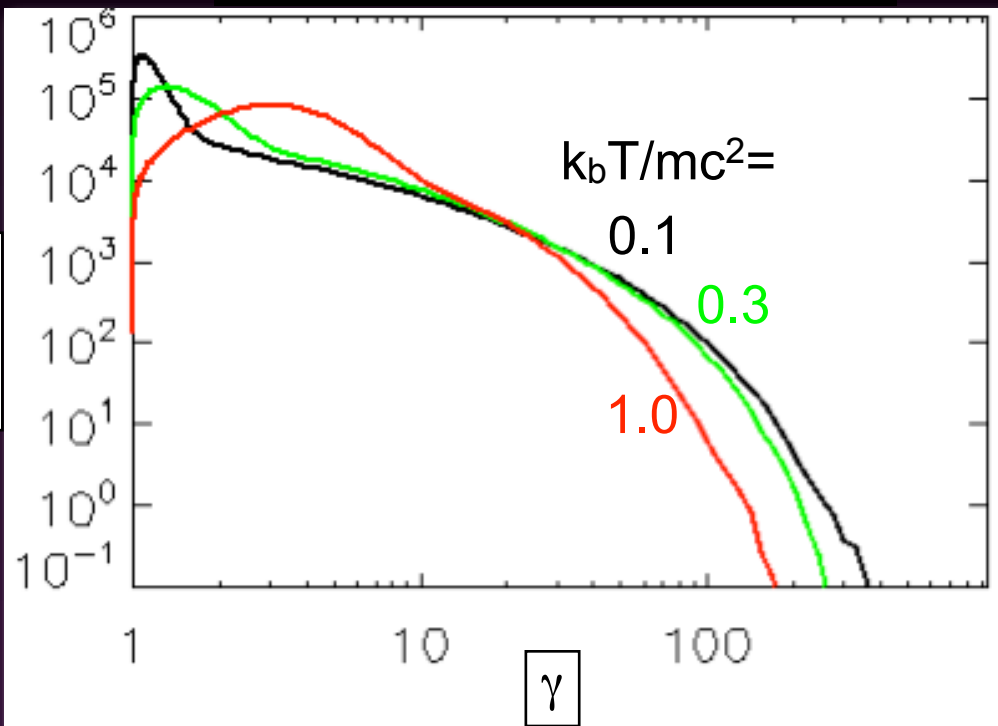
Dependence on the temperature

$$\sigma_w = \frac{B_0^2}{4\pi w}$$

w =enthalpy

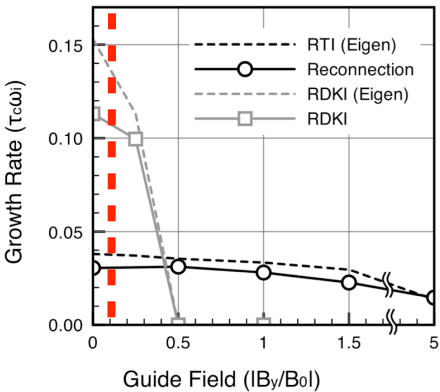
$$w = e + p = nmc^2 + [\Gamma/(\Gamma - 1)]p$$

$\sigma=10$ electron-positron



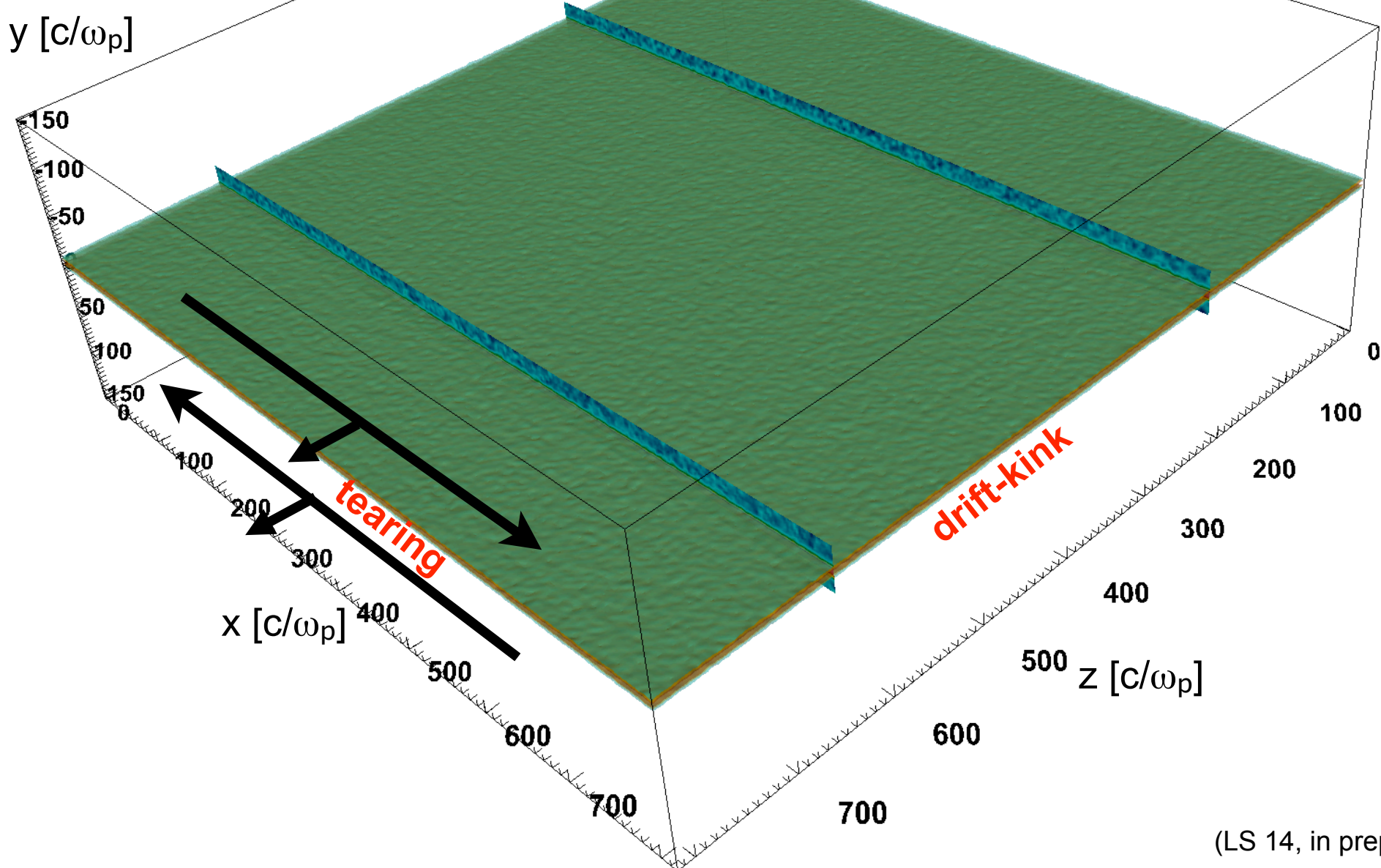
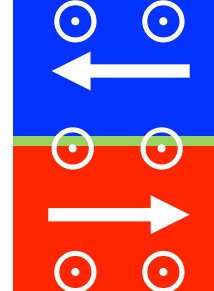
(LS 14, in prep)

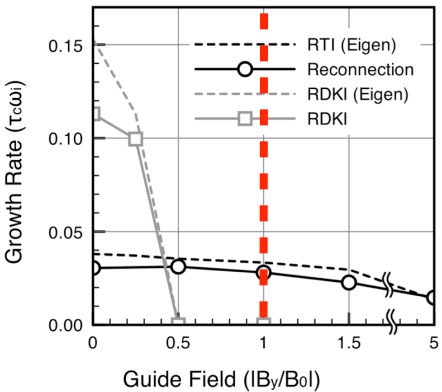
The temperature dependence is encoded in σ_w



$\sigma=10$ $B_g/B_0=0.1$

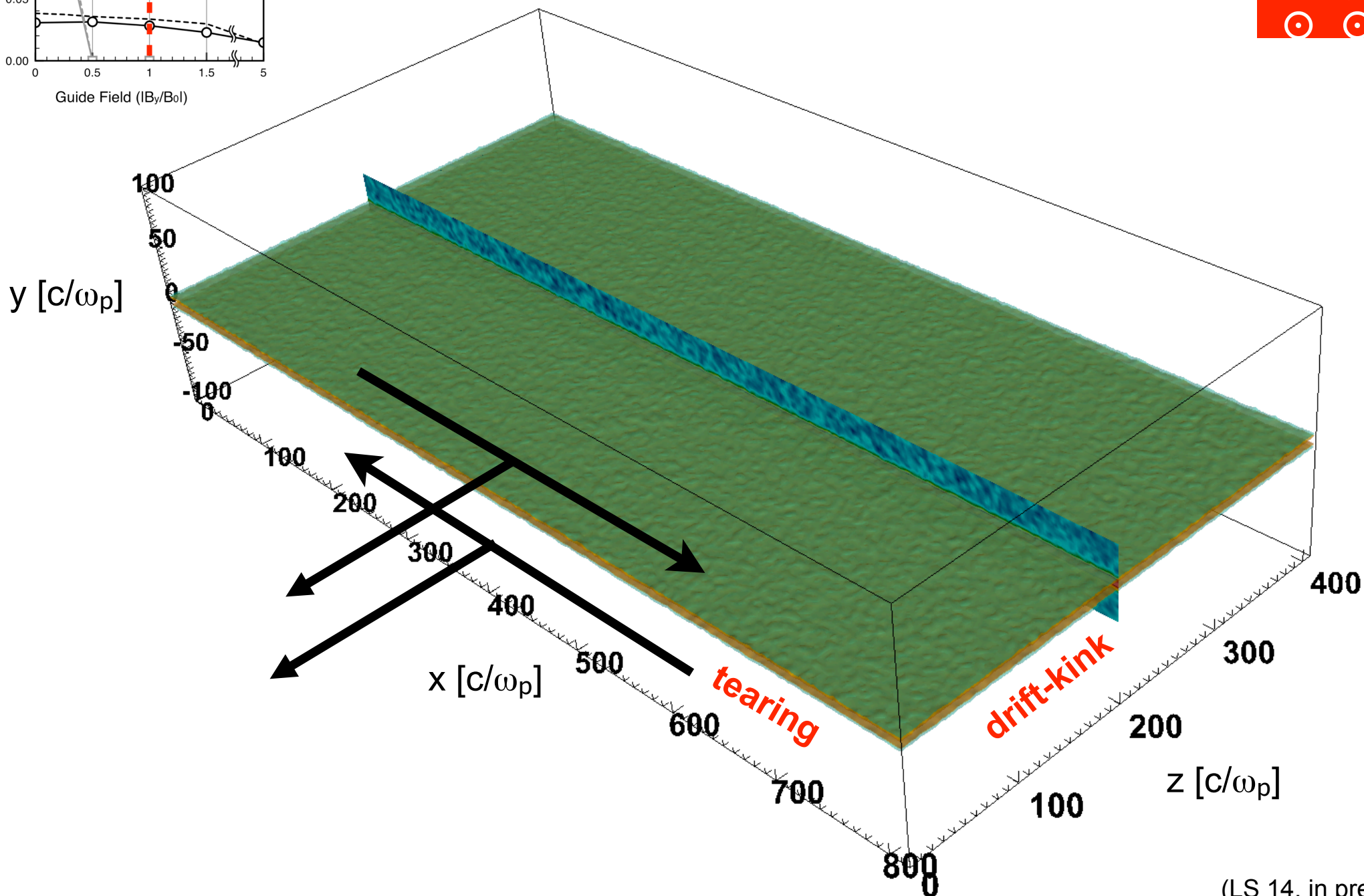
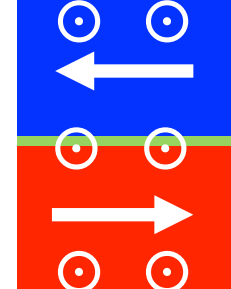
Density



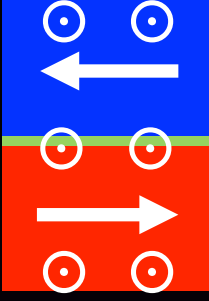


$\sigma=10$ $B_g/B_0=1.0$

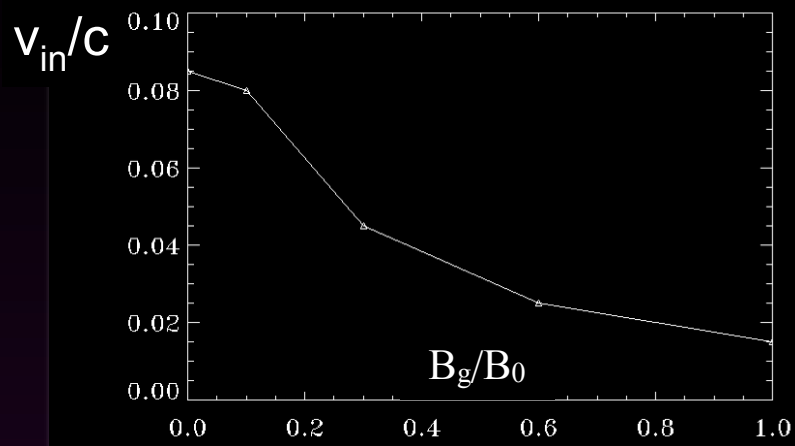
Density



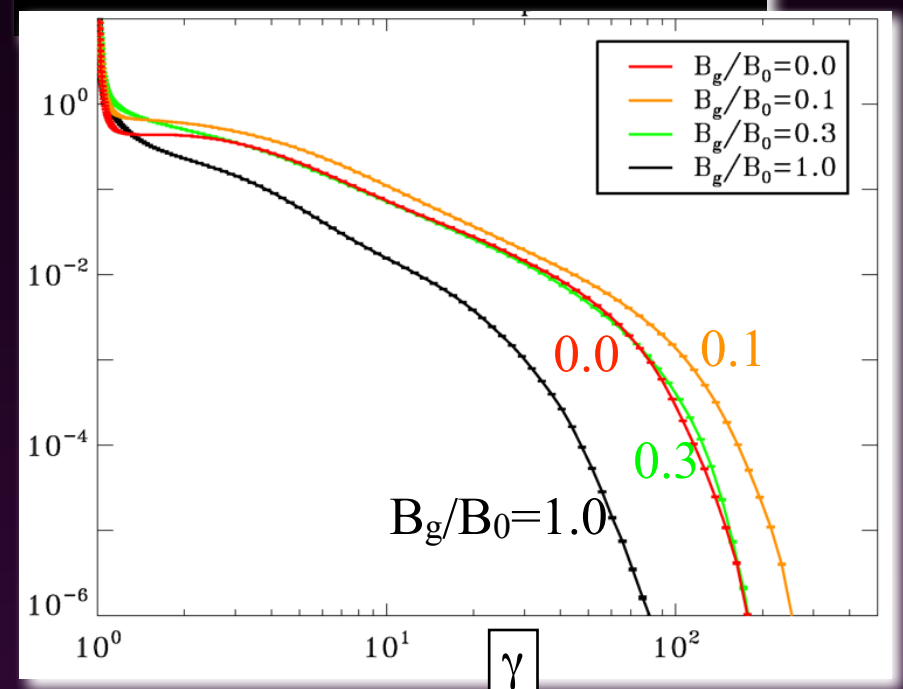
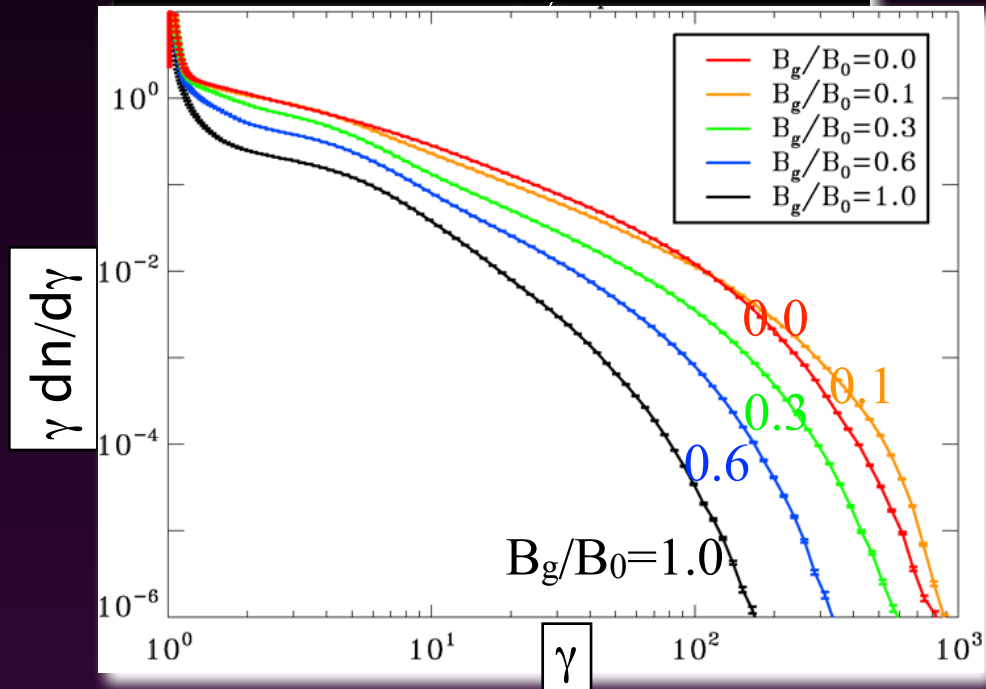
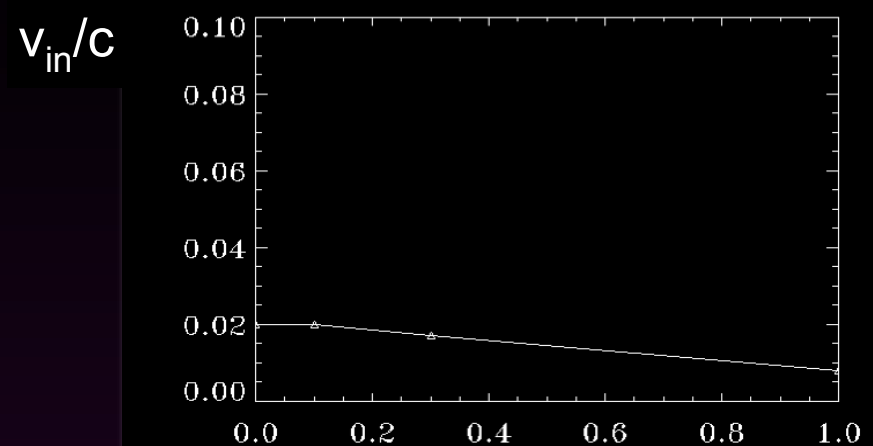
Dependence on the guide field



2D $\sigma=10$ electron-positron



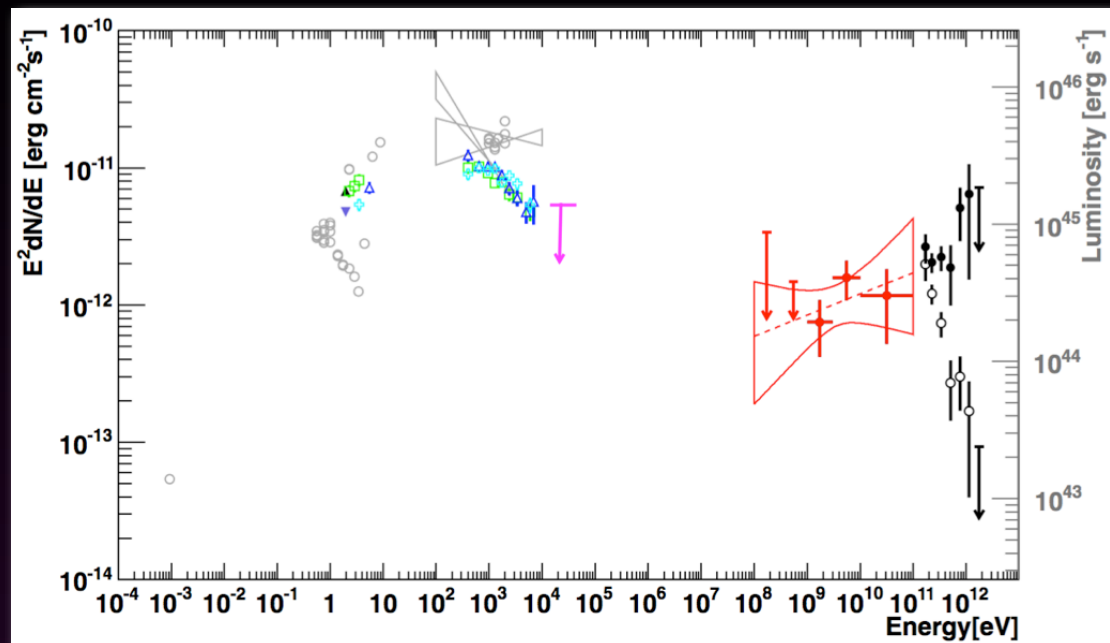
3D $\sigma=10$ electron-positron



For stronger guide fields, the normalization and the maximum energy are smaller, because the reconnection electric field (and so, the reconnection rate) are smaller.

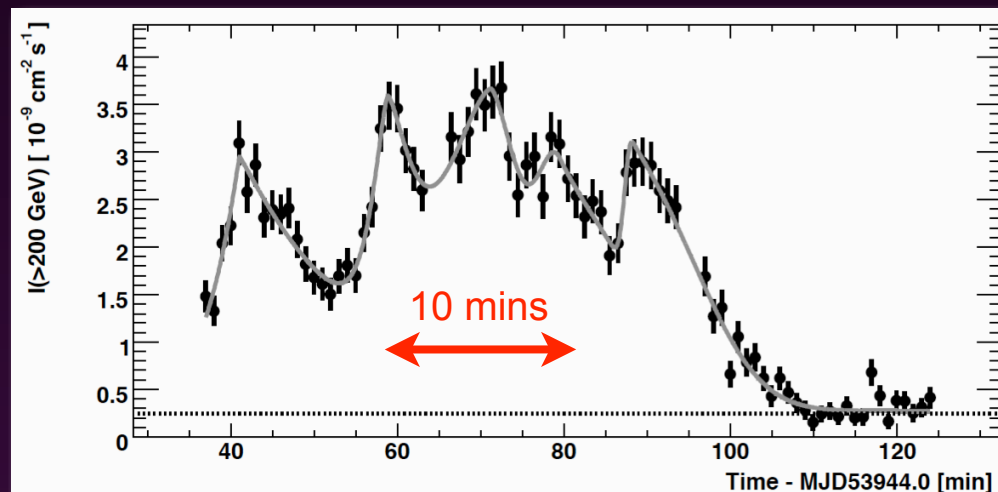
Astrophysical implications

- For high magnetizations, the non-thermal slope can be $p < 2$, as needed to explain the de-absorbed TeV spectra in blazars and the spectrum of the Crab GeV flares.



(HESS 11)

- Small-scale islands in reconnection might explain the fast (~ 10 minutes) variability in TeV blazars and the Crab flares.



(Aharonian et al. 07)

Summary

- Relativistic magnetic reconnection in pulsar winds and magnetically-dominated jets is an efficient particle accelerator, in 2D and 3D.
- Relativistic reconnection can efficiently produce non-thermal particles, in the form of a power-law tail with slope between -2 and -1 (harder for higher magnetizations), and max energy growing linearly in time (promising for UHECRs).
- The reconnection rate (and so, the rate of growth of the max energy) is $\sim 0.1 c$ in 2D and $\sim 0.02 c$ in 3D for the case of zero guide field. In 3D, the drift-kink mode is unimportant for the long-term evolution.
- The reconnection rate increases with magnetization up to $\sim 0.15 c$ (in 2D). It decreases with the strength of the guide field.